8-1-2022

Optimal Design of Functionally Graded Parts

Priyambada Nayak
San Jose State University, priyambada.nayak@sjsu.edu

Amir Armani
San Jose State University, amir.armani@sjsu.edu

Recommended Citation

Priyambada Nayak and Amir Armani. "Optimal Design of Functionally Graded Parts" *Metals* (2022). https://doi.org/10.3390/met12081335

metals

MDPI

Review

Optimal Design of Functionally Graded Parts

Priyambada Nayak * and Amir Armani

Mechanical Engineering Department, San Jose State University, San Jose, CA 95192, USA
* Correspondence: priya.cetb@gmail.com

Abstract: Several additive manufacturing processes are capable of fabricating three-dimensional parts with complex distribution of material composition to achieve desired local properties and functions. This unique advantage could be exploited by developing and implementing methodologies capable of optimizing the distribution of material composition for one-, two-, and three-dimensional parts. This paper is the first effort to review the research works on developing these methods. The underlying components (i.e., building blocks) in all of these methods include the homogenization approach, material representation technique, finite element analysis approach, and the choice of optimization algorithm. The overall performance of each method mainly depends on these components and how they work together. For instance, if a simple one-dimensional analytical equation is used to represent the material composition distribution, the finite element analysis and optimization would be straightforward, but it does not have the versatility of a method which uses an advanced representation technique. In this paper, evolution of these methods is followed; noteworthy homogenization approaches, representation techniques, finite element analysis approaches, and optimization algorithms used/developed in these studies are described; and most powerful design methods are identified, explained, and compared against each other. Also, manufacturing techniques, capable of producing functionally graded materials with complex material distribution, are reviewed; and future research directions are discussed.

Keywords: functionally gradient material; design optimization; additive manufacturing; finite element method; material modeling

Citation: Nayak, P.; Armani, A. Optimal Design of Functionally Graded Parts. *Metals* **2022**, *12*, 1335. https://doi.org/10.3390/met12081335

Academic Editor: João Pedro Oliveira

Received: 1 July 2022
Accepted: 4 August 2022
Published: 10 August 2022

1. Introduction

Functionally Graded Materials (FGM) are a type of composite materials made of two or more constituent phases with a continuously changing phase distribution throughout the volume [1,2]. Typically, constituent phases are two materials with distinct thermo-mechanical properties, the volume fraction of each of which changes gradually throughout the part. Many research efforts have been carried out to develop accurate mathematical models and numerical techniques for homogenization of FGMs, predict their responses to mechanical and thermal loads, propose testing methods to measure their properties, and invent new manufacturing processes to build FG parts. Several journal articles and book chapters have been written to review these efforts (e.g., [3–14]).

Most of the above-mentioned works are limited to simple one-dimensional material gradient. However, with the advent of Additive Manufacturing (AM) techniques, complex three-dimensional material composition distributions are also achievable. Vaezi et al. [15] have published a review paper on multiple-material additive manufacturing. Also, a detailed review of AM methods, materials and their potential applications can be found in [16,17]. Accordingly, many researchers developed models to represent FGMs with complex material composition distribution. Kou and Tan [18] have published a review paper on this topic. These representation techniques need human input for material composition at certain object features (points, curves, surfaces, etc.) and do not result in optimal material composition distribution. The early developments on the processing

and thermo-mechanical behavior of FGMs are well described in a two-part review paper by Mortensen and Suresh [19,20]. By the turn of the century, the increased research on the modelling and analysis of FGM structures led to several more reviews. One of the first by Birman and Byrd [13] addressed a variety of FGM-related aspects, including the homogenization of particulate-type FGMs, the thermoelastic modelling and analysis of FGM structures, manufacturing issues, and fracture problems in FGMs.

Since late 1990s, researchers have developed methods to optimize the material composition distribution in FG parts. These methods determine the material composition at each point to achieve a certain objective (e.g., minimizing residual thermal stress). They consist of four building blocks: homogenization of FGM, representation of FGM, finite element analysis, and optimization. This paper, for the first time, reviews FGMs with optimal design, their design methodologies, manufacturing techniques, and future directions.

2. Evolution of Design Methods

The performance of an FGM is not only a function of properties of its constituent phases, but it is also directly associated with the ability of a designer in using materials in the optimal manner. The following sections provide a chronological overview of research on the optimal design of various types of FG components, as well as an overview of the evolution of methodologies created to optimize the material composition distribution in FG parts.

2.1. Prior to 2002

In 1972, Bever and Duwez [21], and Shen and Bever [22] proposed the concept of gradation in material composition for composite polymeric materials. Their efforts, however, had a limited impact, owing to the unavailability of viable production processes at the time. In 1984, the National Aerospace Laboratory of Japan developed FGMs for advanced ultra-high temperature resistance structural materials to be used in space structures, fusion reactors, and spaceplanes, as well as various functional applications (e.g., optics and electronics). Their first national project on FGM was carried out from 1987 to 1991 and FGM test samples for the base of spaceplane fuselages and hemispherical bowls for nose-cones were fabricated [6,23–25]. The second national project was launched between 1993 and 1998 with the goal of improving the energy conversion efficiency of FG structures and fabricating thermoelectric and thermionic materials [24,25]. The "physics and chemistry of FGMs" project was carried out in 1996–1999 to address the fundamental challenges of grading physical and chemical properties, and it was a huge success in boosting FGM research and applications [25]. Since then, FGMs have evolved dramatically. Some milestone achievements are shown in Figure 1.

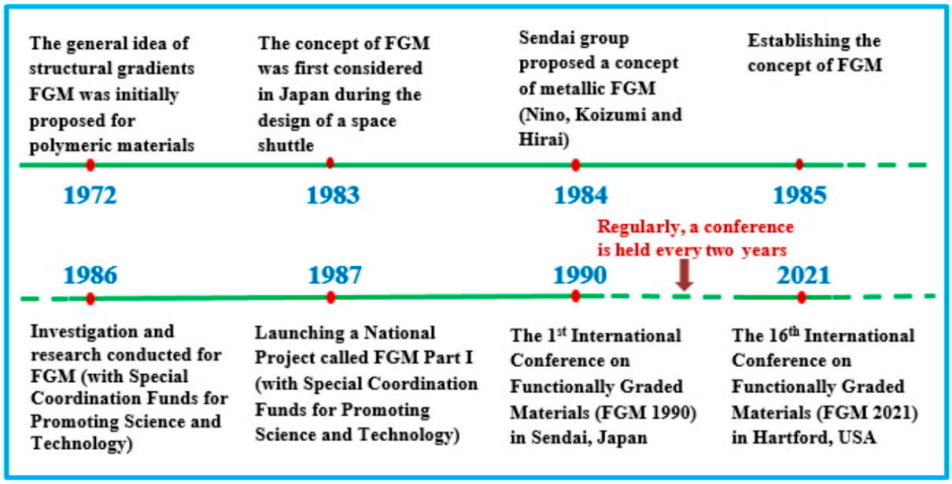

Figure 1. Historical overview of relevant milestones in the research and development of FGMs. "Reprinted with permission from [26]. Copyright 2020 Elsevier".

Gradation in microstructure played an essential part in the evolution of FGMs, and FGMs were divided into three categories based on the distribution of constituent phases, namely continuous, discontinuous (step-wise or layered), and multiphase gradation. Figure 2 depicts different forms of FG microstructures. Many authors analyzed FGM problems with one-dimensional material properties, in many different cases, under mechanical and/or thermal loads (e.g., Noda and Tsuji [27], Arai et al. [28], Erdogan et al. [29], and Noda and Jin [30]). Their results were very motivating and enhanced their aims in the development of new high-temperature materials. The temperature distribution in most machine elements in practical cases changes in two or three directions. Therefore, if the FGM has two- or three-dimensional dependent material properties, more effective high-temperature resistant materials can be obtained. Accordingly, bi-directional FGM whose material properties are dependent in two directions were introduced. Many studies on 2D-FGM have been conducted (e.g., Clements et al. [31]; Nemat-Alla and Noda [32–34]; Marin [35]; Ke and Wang [36]). Unfortunately, for continuous gradation of material properties, they have all considered exponential functions. Except at the upper and lower surfaces of FGM, the use of exponential functions for material properties frequently aids the analytical solution but does not provide true representation for material properties.

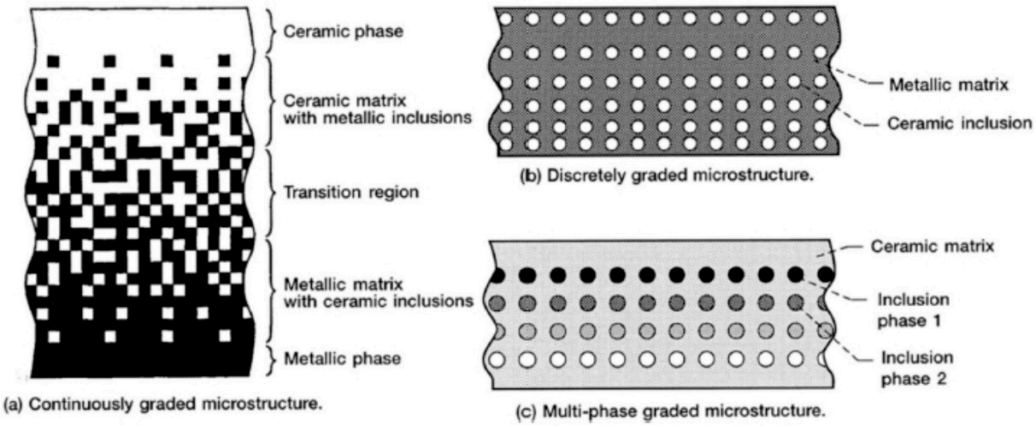

Figure 2. Different types of FG microstructures. "Reprinted with permission from [37]. Copyright 1999 Elsevier".

Aboudi et al. [38,39] investigated the behavior of FGMs using thermo-elastic/plastic theory. Their research avoided the drawbacks of the traditional micromechanical technique used in the examination of FG composites. For relaxing the effective thermal stress, Cho and Ha [40] adjusted the volume fractions distributions of FGM. For the FGM, they found the best volume fractions distribution in two directions. The optimum volume fractions obtained have a random distribution, which is far more difficult to model or simulate than traditional FGMs, which have continuous composition fluctuations. Goupee and Vel [41] suggested a two-dimensional modeling and optimization methodology for FGM material composition distribution. The element-free Galerkin approach was used to solve two-dimensional quasi-static heat conduction and thermo-elastic problems. By piecewise bi-cubic interpolation of volume fractions specified at a finite number of grid points, they were able to derive the spatial distribution of ceramic volume fraction.

2.2. 2003–2009

Nemat-Alla [42] proposed the addition of a third material ingredient to the typical FGM to survive the resulting severe heat stresses. The resulting material was a 2D-FGM with the addition of mixture rules and volume fractions relationships. When comparing 2D-FGM to conventional FGM, it was discovered that 2D-FGM had a greater ability to minimize thermal stresses than conventional FGM. It's worth noting that the temperature-independent characteristics and elastic behavior of FGMs have been taken into account in the majority of the above-mentioned studies. Nemat-Alla et al. [43] investigated the

temperature dependent properties and elastic-plastic behavior of 2D-FGMs under severe thermal loading. They proposed a 3D finite element model of 2D-FGM plates with temperature dependent non-linear material properties. The analysis also includes an elastic plastic stress–strain relationship based on the rule of combination of the 2D-FGM.

For FGMs, it is possible to vary the material composition arbitrarily during production, and therefore the problem of optimization of non-homogeneous material composition to minimize the thermal stress has attracted the interest of numerous researchers. For such problems of material composition optimization, Noda and his coworkers [27,44–46] analyzed one-dimensional problems for a steady state of a nonhomogeneous plate, a hollow circular cylinder and a hollow sphere. However, with regard to thermal stress problems, it is well-known that maximum stress distribution occurs in a transient state which lasts from the beginning of the heating to the steady state, in general. Therefore, for such optimization problems, it is necessary to consider the transient state in which the maximum stress distribution is predicted to occur.

Tanigawa et al. [47] analyzed one-dimensional optimization problem of material composition of a nonhomogeneous plate in a transient state, for the first time. In a subsequent paper, Tanigawa et al. [48] carried out the optimization of material composition of a nonhomogeneous hollow circular cylinder in a transient state to reduce the thermal stress distributions. These optimization problems have been treated by making use of the nonlinear programming method. However, when such a nonlinear programming method is adapted to the optimization problem, the analytical procedure becomes complicated and, hence, a long central processing unit (CPU) time for the numerical calculations is needed. On the other hand, the concept of neural networks has been introduced to analytical procedures of structural optimization [49–51] and to inverse problems [52]. It is well known that a neural network can be constructed by a comparatively simplified procedure for numerical calculations, and optimum calculation can be carried out without nonlinear programming method by making use of Tanaka's method [53]. As a result, compared to when nonlinear programming is utilized, the optimal solution can be produced in a relatively short amount of time on the CPU. There are several papers on optimization of material composition for FGM using neural networks (e.g., [54–57]).

Research pertaining to the optimization of FGMs is comprised almost entirely of single-objective studies [40,57–63]. However, the design of practical FGM structures often require [64] the maximization or minimization of multiple, often conflicting, objectives. The first study considering multi-objective optimization of FGMs was performed by Huang et al. [65]. They used a weighted Tchebycheff approach to do a bi-objective optimization design of FG flywheels with general one-dimensional grading profiles and radially changing thicknesses. Goupee and Vel [66] developed a methodology for the multi-objective optimization of material distribution that is based on the element-free Galerkin (EFG) method [67] for the numerical simulation of FGMs. The material composition profile was optimized using a real-coded elitist non-dominated sorting genetic algorithm. In a subsequent paper, Vel and Goupee [68] applied the same algorithm to optimize the volume fraction of a two-dimensional cooling component made of tungsten and copper. Both transient and steady-state conditions were considered. Thus, the problem was a bi-objective optimization problem. They optimized the volumetric fraction only at eight nodes and for adjacent points it was obtained using a range-restricted piecewise bi-cubic interpolation.

In [69], teeth made of HAP/Col (ceramic) and titanium under applied chewing forces were considered. The goals were to maximize cortical and cancellous bone densities while minimizing the vertical displacement. The material gradient was only in vertical direction and governed by a power law, $V_c = (y/h)^m$. There was only a single real-value parameter (m) to be optimized and a simple optimization algorithm was utilized as follows. All three objective functions were approximated by polynomials in "m" and a least square method was applied to determine the unknown coefficients of the polynomials. In addition, the weighted average method was used to solve the multi-objective optimization problem.

Cheng and Batra [70] presented a 3D analytical closed-form solution for the thermo-mechanical deformations of an isotropic, FG elliptic plate. The through-thickness variation of the volume fraction of the ceramic phase in a metal-ceramic plate was assumed to be given by a power-law function, while the effective material properties were obtained by the Mori-Tanaka [71] approach. Praveen and Reddy [72] investigated the transient nonlinear thermoelastic behavior of an FG ceramic/metal plate, applying the von Karman plate theory and the Finite Element Method (FEM). It was found that the general response of a plate with material properties between those of ceramic and metal is not intermediate to the responses of ceramic and metal plates. A 3D analytical solution for the thermo-mechanical response of simply supported FG rectangular plates was given by Reddy and Cheng [73], using an asymptotic expansion method. The locally effective material properties were estimated by the Mori-Tanaka scheme. In this paper, temperature, displacements and stresses of the plate were computed for different volume fractions of the ceramic and metallic constituents. Turteltaub [62] formulated the temperature optimization problem as finding a distribution of material properties (volume fraction of the constituent phases) that minimizes the difference between the target and actual temperature distributions. The other paper by the same author illustrated that the loading history is important in optimization problems, even if the material remains in the elastic range [61]. Carrera et al. [74] addressed the static response of FG plates subjected to transverse mechanical loads. Applying Carrera's Unified Formulation (CUF) [75], originally developed for multilayered structures and for the principle of virtual displacements (PVD), closed form and FE solutions were derived.

2.3. 2010–2015

Most researchers have employed linear shape functions for capturing the material gradations inside elements in the graded finite element context in optimization problems, even though the solution is approximated by higher order shape functions. For the topology optimization of FG beams subjected to thermal and mechanical loads, Almeida et al. [76] used the Continuous Approximation of Material Distribution (CAMD) approach. Their goal was to identify the best material distribution for such materials that would result in the beams having the least amount of compliance. To deal with uncertainty in the manufacturing process, a reliability-based design optimization for FGMs was proposed by Noh et al. [77]. They considered a finite number of volume fractions of homogenized FGM layers and material properties as random variables, with statistical information such as mean, standard deviation, and statistical distributions. They assumed a gradient from metal to ceramic in four layers as shown in Figure 3. This technique simplifies the FEA to a great extent as there is no need to model an FG part, but only a few homogeneous materials need to be modeled and assembled.

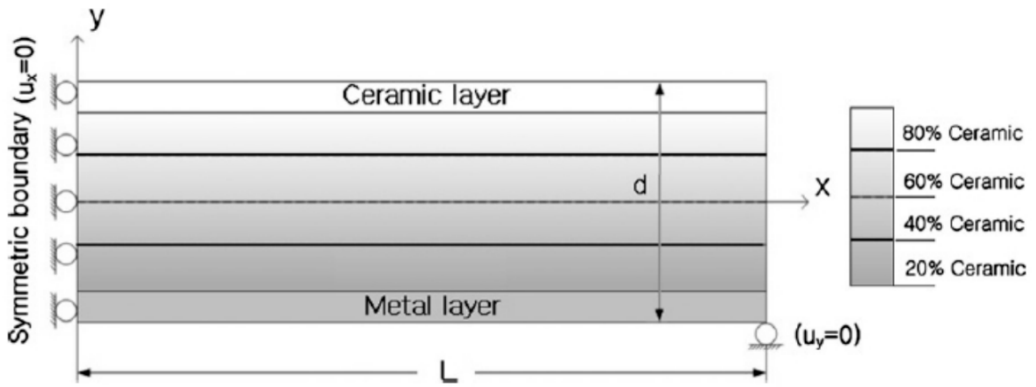

Figure 3. Example of FG part composed of discrete homogenous layers. "Reprinted with permission from [77]. Copyright 2013 Elsevier".

Nabian and Ahmadian [78] used a GA-based optimization strategy to concurrently minimize the mass and maximize the first natural frequency of a FG hollow cylinder.

They assumed that the material properties vary continuously through the thickness of the cylinder (one-dimensional gradient in the radial direction) and formulated the first natural frequency as well as its mass in terms of the volume fraction of the constituents. Nouri and Astaraki [79] optimized the volume fraction distribution of materials and geometry of FG cylindrical shells via GA to maximize the sound transmission loss based on the first resonant frequency. Constraints included the weight, frequency range, and thickness of the shell structure. In this study, they looked at a variety of materials and discovered that the combination of nickel-aluminum and steel-aluminum provided the best sound transmission loss and the lightest weight.

Xu et al. [80] minimized the thermal residual stresses induced in C/SiC FG coating of carbon/carbon (C/C) composites when cooling down from the processing temperature by controlling the thicknesses and compositional distribution of the C/SiC FGM. They implemented a one-dimensional analytical model based on force and moment balances to determine the thermal residual stresses and found an optimal design using a particle swarm optimization (PSO) algorithm. Figure 4 gives a schematic description of the C/SiC FGM system, where *N* coating layers are deposited on the substrate. Kou et al. [81] utilized Particle Swarm Optimization (PSO) to optimize one-dimensional and two-dimensional material distribution of parts exposed to temperature variations. The objective of optimization for the main example problem was to simultaneously minimize the von Mises stress and the mass of a plane made of zirconia (ZrO_2) and titanium alloy (Ti-6Al-4V). The major novelty of this paper is to use an advanced representation model for heterogeneous parts which is a feature tree-based procedural model.

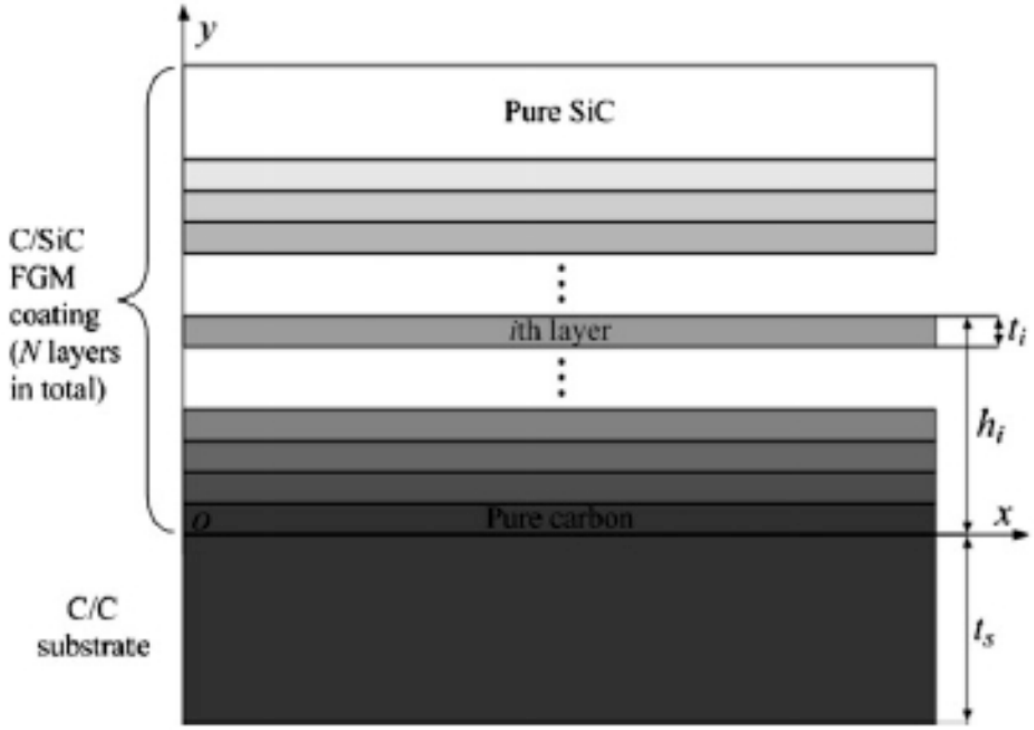

Figure 4. Schematic description of the C/SiC FGM system. "Reprinted with permission from [80]. Copyright 2012 Elsevier".

Optimization of material composition of FGMs based on multiscale analysis method that can efficiently predict the microscopic stress state (namely, the asymptotic expansion homogenization (AEH) method) was conducted by Chiba and Sugano [82]. They optimized the material composition of an infinite FG plate made of Ti and ZrO_2 in only one direction using a genetic algorithm. The AEH method has the advantages that the equivalent macroscopic material properties for composite materials with an arbitrary complicated mi-

crostructure can be calculated exactly and the distribution of stresses in the microstructure can also be evaluated.

Ghazanfari and Leu [83] used a sequential approximate optimization method to maximize the stiffness of beams with two-dimensional material distribution. The optimization constraint was the total mass of the beam predetermined by the user. They used the linear rule of mixture [84] to estimate all material properties and developed their own finite element code to the strain analysis. Although their results showed a considerable increase in the stiffness of the beams after optimization as compared to the beams with uniformly distributed materials, it was infeasible to employ their technique for other objective functions.

FGMs have a number of features that have enticed researchers to use them in biomedical applications. Bahraminasab et al. [85] carried out a multi-objective design optimization of an FG femoral component using FEA and response surface methodology. Their objective was to extend the lifespan of femoral component of a total knee replacement. The performance measures of the FGM design included: (1) the stress distribution on the distal femur to avoid stress shielding effect, (2) the contact characteristics of tibia insert (contact area and pressure) to avoid wear and (3) micro-motion at the implant/bone interface to avoid instability. The results of using optimized FGM were compared with the use of standard Co–Cr alloy in a femoral component to demonstrate relative performance.

2.4. 2016–2022

Many researchers carried out extensive studies relating to thermal stress analyses and heat transfer problems in FGMs during past decades. However, in recent years, the thermo-mechanical response of FGM structures has gained more attention due to the recent developments and emerging new applications of FGMs. Some works on optimization of FGM structures under thermo-mechanical loadings are mentioned herein. Lieu and Lee [86] developed a novel metaheuristic algorithm known as adaptive hybrid evolutionary firefly algorithm (AHEFA) to optimize the material distribution of aluminum and zirconia FG plate under thermo-mechanical loads. The objective was to minimize the compliance under ceramic volume constraints. The static analysis of FG plates was carried out using a non-uniform rational B-splines (NURBS) based isogeometric finite element model in conjunction with the third-order shear deformation theory (TSDT). The material distribution via the B-spline basis functions was represented using Greville abscissae to define the coordinates of the specified ceramic volume fractions along the plate thickness at a set of control points.

A work by Correia et al. [87] focused on the optimization study of FG plates considering several objectives, such as the mass and material cost minimization, natural frequency maximization, and minimization of stress. The design variables were the index of the power-law distribution in the metal-ceramic graded material, the thicknesses of the FGM layer, and the face sheets while manufacturing limitations were also taken into account. Most importantly, the multi-objective optimization problems were solved by a rather efficient Direct Multi-Search (DMS) derivative-free method. A multi-objective optimization procedure based on DMS was also adopted in Moleiro et al. [88] work for the design optimization of FG plates under thermo-mechanical loadings. The objective functions were to minimize mass, deformation, and stress altogether. They used the layer-wise mixed model for the thermo-mechanical analysis of multi-layered FG plates and Tsai-Hill failure criterion. Most recently, Qu et al. [89] developed a new FG magneto-electro-elastic composite microbeam model using a general higher-order deformation theory (GHDT) to account for the symmetric thickness-shear and thickness-stretch deformations of a beam and a modified couple stress theory to describe the microstructure-dependent size effect.

The advances in manufacturing processes inspired the researchers to consider the development of porous biomaterials with a functional gradient and optimizing the porosity pattern in these materials. Implementing an optimization algorithm based on mechanobiological criteria, Boccaccio et al. [90,91] developed FE models for FG scaffolds. The finite element model of FG scaffold is shown in Figure 5. They used a sequential quadratic

programming method to maximize the percentage of scaffold volume occupied by bone. The simulation results revealed that rectangular and elliptic pores could facilitate a large number of tissue growth compared to circular pores, and the fastest-growing bone tissue was found at the location of largest curvature. These studies proved to be an efficient way for the optimization of FG scaffolds, when biological loading condition is considered.

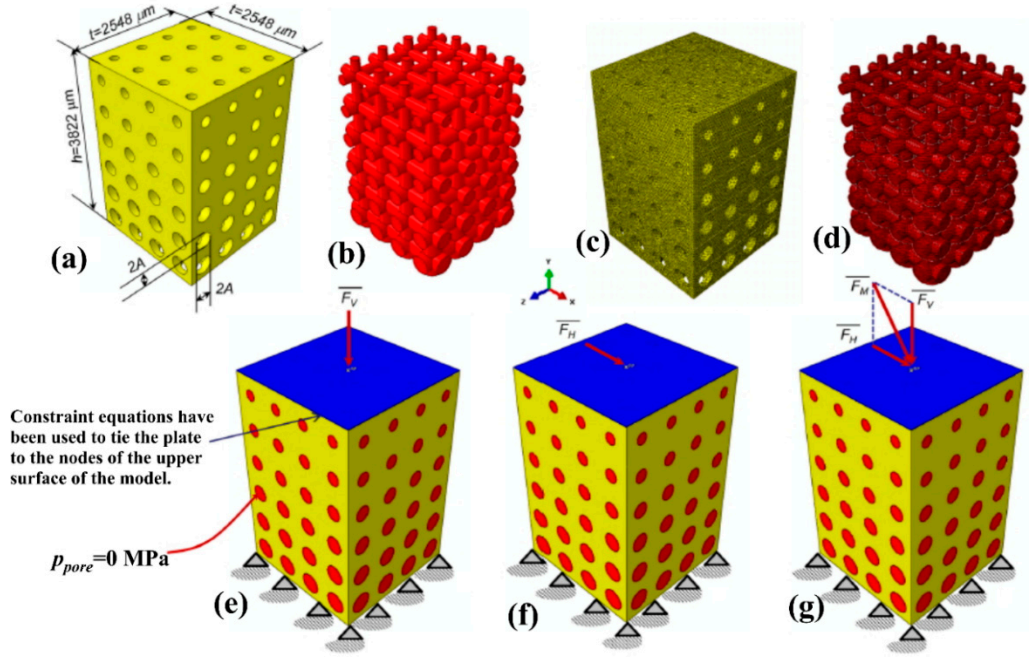

Figure 5. Parametric finite element model of the FG scaffold. "Reprinted with permission from [90]." CAD model (**a**,**b**) and finite element mesh (**c**,**d**) of the scaffold (**a**,**c**) and granulation tissue (**b**,**d**). The nodes of the bottom surface of the model were clamped (**e**–**g**) while those of the upper surface were tied to a rigid plate (represented in blue).

Topology optimization has been a popular method to design mechanically efficient cellular materials. A multi-physics topology optimization of FG controllable porous structures, while improving heat dissipation at the same time, was carried out by Das and Sutradhar [92]. Porous cells (random architecture) were employed instead of lattices (ordered architecture) in this approach, with pore size and relative density as design variables. A sensitivity-based controlling scheme was presented, which can offer graded porous structures with variation in member and pore size in different sensitive zones. The research based on multi-objective topology optimization can impart improved functionality in the creation of bio-scaffolds for hip implants (Wang et al. [93]), the design of aerospace structures (Aage et al. [94]), on improving the contour of the blades in the field of turbomachinery (Lee et al. [95]). Some studies have tried to improve the material layout or reduce the mass of turbine blades (Magerramova et al. [96]).

3. Homogenization Approaches

The constituent phases of FGMs (e.g., ceramic and metal particles) are of arbitrary shapes and mixed up in arbitrary dispersions. Therefore, prediction of their effective material properties at a point by knowing the volume fractions of the constituents is not generally a simple task. Different strategies have been proposed for this purpose thus far, each of which may work well for a certain type of problems depending on the fabrication process and shapes of the constituent particles. Generally, FGMs are designed to suit high-temperature conditions because the ceramic constituent provides high thermal resistance and hence most of the commonly-used FGMs are made of ceramic and metal. Homogenization techniques are essentially required to derive the effective properties

of macroscopic homogeneous composite materials from the microscopic heterogeneous material structures.

Some researchers did not use any homogenization approach. Instead, they directly optimized the distribution of material properties, not material composition. For example, Zhang et al. [97] found the optimal distribution of the Young's modulus across the part. The advantage of this approach is its simplicity, but it cannot be used if more than one material property is needed. For instance, if the Young's modulus and the coefficient of thermal expansion are needed to solve a problem, this approach cannot be implemented. In addition, if the final part is to be fabricated via any manufacturing technique, the optimal material property distribution needs to be converted to material composition distribution and a homogenization method must be implemented.

Several homogenization models, viz. rule of mixtures (Voigt Scheme), Mori-Tanaka method, Levin's model, effective medium theory, Maxwell model, reciprocity model, Tamura model, and finite element-based models are available in literatures [3] to compute the effective material properties. There are many homogenization methods in general, but the present paper focuses on the homogenization methods used in the material distribution optimization studies. For evaluating FG structures, researchers recommend the Voigt and Mori–Tanaka models among the homogenization models. It is simple to compute the upper and lower bounds of effective material properties of a heterogeneous material using the Voigt model. It is also computationally more efficient compared to Mori–Tanaka method [98]. Several such models based on the micromechanics method and effective medium approximation have been developed and reported in the literature over the years and are presented in this section.

3.1. Rule of Mixture

The most popular homogenization approach is the rule-of-mixture in which a material property at a point is estimated by the volume weighted average of the properties of its constituents. In this method, each effective material property is only dependent on the corresponding material property of the metal and ceramic phases and the volume fractions. The advantage of this method is that it is easy to calculate and can be considered as the upper and lower bounds for the effective elastic properties of a heterogeneous material [99].

The effective material properties P (e.g., Young's modulus E, Poisson' ratio ν, coefficient of thermal expansion α, and thermal conductivity k) may be expressed as

$$P = P_1V_1 + \mathrm{P}_2V_2 \tag{1}$$

where, P_i and V_i are material properties and volume fraction of phase i, respectively. Thus, having properties of each material, one could calculate the effective properties for any composition (clearly, at each point, $V_1 + V_2 = 1$).

The rule of mixture is simple and widely used to characterize the effective material properties of FGMs [88,100,101]. Although this simple rule is accurate for a fiber reinforced composite that is aligned in the loading direction and deformed under iso-strain conditions, the reliability of this method has been known to be highly questionable, because it does not include the details on particles and dispersion layout as well as the interaction effect between the constituents [102]. As a result, designers are looking for more precise estimates of the Young's modulus and thermal expansion coefficients, which are the most important factors in the thermoelastic response of FGMs.

3.2. Mori-Tanaka Scheme

Mori–Tanaka [71] scheme is also widely employed in the literature and is believed to yield promising estimations of effective material properties in typical realistic problems. In Mori–Tanaka scheme, extracting the effective material properties is based on the distributed small spherical particles (metal phase) into matrix (ceramic phase). According to the Mori-

Tanaka method, the effective bulk modulus (K), and the effective shear modulus (μ) of a mixture of two constituents is given by:

$$\frac{K - K_1}{K_2 - K_1} = \frac{V_2}{1 + (1 - V_2)[3(K_2 - K_1)/(3K_1 + 4\mu_1)]} \tag{2}$$

$$\frac{\mu - \mu_1}{\mu_2 - \mu_1} = \frac{V_2}{1 + (1 - V_2)(\mu_2 - \mu_1)[\mu_1 + \mu_1(9K_1 + 8\mu_1)/6(K_1 + 2\mu_1)]} \tag{3}$$

where K_i, and μ_i are bulk Modulus and shear Modulus of phase i, respectively. Subsequently, the effective Young's modulus (E) and Poisson's ratio (ν) are obtained as $E = 9K\mu/(3K + \mu)$ and $\nu = (3K - 2\mu)/(6K + 2\mu)$, respectively.

This model has been applied to many cases in literature, Hirshikesh et al. [103] presented a phase field modeling for crack propagation in FGMs. They have used the Mori–Tanaka homogenization theory to calculate the Young's modulus and Poisson's ratio and the rule of mixtures to compute the energy release rate. Srividhya et al. [104] compared Mori–Tanaka and Voigt model through the static analysis of FGM plates. They have observed that the effective elastic properties estimated by the Voigt model are larger than those obtained with the Mori–Tanaka scheme. The difference varies with the change in power-law index n and is seen to be the highest for n = 0.5 to the tune of 11.5%. It has been also observed that the rule of mixtures gives a better estimate of the elastic properties for values of n = 0–2.0, whereas Mori–Tanaka method predicts the elastic properties quite accurately for values above n = 2.0. For a two phase composite, the predictions by Mori–Tanaka scheme lies in between the Hashin-Shtrikman bounds [105], but for the case of multi-phase composites the Mori–Tanaka scheme seems to violate the bounds and thus it is not always practicable for multi-phase composites [106]. Although Mori–Tanaka approach takes into account the stress perturbation inside the matrix due to the presence of other inclusions, it is not able to account for the spatial distribution. So, recently, numerical homogenizations such as finite element approach has been applied for composite system having higher geometric complexities [107], discussed later in this section.

3.3. Levin's Model

Because of the variable thermal fields often found in functionally graded material applications, it is important to also consider estimates of the coefficient of thermal expansion. For a two-phase composite, Levin [108] gives relations for the effective coefficient of thermal expansion (α) in terms of constituent properties, and the effective bulk modulus (K) as

$$\alpha = V_1\alpha_1 + V_2\alpha_2 + \frac{\alpha_2 - \alpha_1}{\frac{1}{K_2} - \frac{1}{K_1}}\left(\frac{1}{K} - \left(\frac{V_1}{K_1} + \frac{V_2}{K_2}\right)\right) \tag{4}$$

where α_i is the coefficient of thermal expansion of ith phase. Thus, having coefficients of thermal expansion of each material, one could implement K from Equation (3) into Equation (4) and calculate the effective thermal expansion coefficient for any composition. So, the availability of an efficient elastic homogenization model is a key requirement for a successful evaluation of the effective coefficients of thermal expansion of composites. Recently, Lages and Marques [109] presented a study about thermoelastic homogenization of two-phase periodic composite materials using an elastic micromechanical model based on the equivalent inclusion approach [110], together with the Levin's formula for evaluation of overall thermal expansion coefficients.

3.4. Maxwell Scheme

To predict the effective thermal conductivities of composite materials, the factors, including the thermal conductivity, size, and distribution of the inclusion, that may affect the effective thermal conductivities should be considered [111]. The effective medium theory [112] is one of the traditional methods to predict the effective thermal conductivities of composite materials. The effective medium theory provides simple analytical models

that can quickly estimate the effective thermal conductivities of the composite materials, knowing the properties and volume fractions of the inclusions [113]. For example, Maxwell [114] was the first person to give analytical expressions for effective thermal conductivities of composite materials. Maxwell scheme appears to be one of the best homogenization techniques in terms of its applicability to cases of anisotropic multiphase composites and accuracy. In his original work, Maxwell calculated effective conductivity of a composite consisting of a matrix material with conductivity k_0 and isolated spherical inhomogeneities of conductivity k_1 and volume fraction V. For this aim, he considered a large sphere of unknown effective conductivity k_{eff} and calculated the far-field asymptotics of the perturbation of the externally applied electric field in two different ways: as (1) a sum of far-fields generated by the small spheres, and (2) the far-field generated by the large sphere. Equating the two, yields the effective conductivity in the following form: equation:

$$k_{eff} = k_0 \frac{1 + 2V\Psi}{1 - V\Psi} \tag{5}$$

where, $\Psi = (k_1 - k_0)/(k_1 + 2k_0)$.

This approach is probably the oldest homogenization technique. Interestingly, over one-and-a-half century from its publication, the Maxwell's scheme continues to give rise to intensive discussions in literature. In a recent work, Sevostianov and Bruno [115] adopted Maxwell homogenization scheme to evaluate residual stresses in multi-phase (and eventually anisotropic) materials. They concluded that Maxwell scheme, being applied to the calculation of the residual stresses in composites, showed good agreement with the experimental results. Simplicity of the Maxwell scheme seemed to be attractive for many authors, and in a number of works the method was applied to calculation of effective conductive and elastic properties of composites with ellipsoidal inclusions and even hybrid composites containing different families of ellipsoidal inclusions [116]. The Maxwell technique produces the same equations for the effective elastic constants as previous homogenization approaches that appear to take into account interactions between inclusions in elastic composites with spherical inclusions (e.g., the effective field method and Mori–Tanaka method [117]). As a result, there was a belief that the Maxwell scheme's conclusions may be extended to the region of large volume fractions of inclusions. Maxwell's approach can also be generalized to other physical properties such as piezoelectricity [118]. The drawbacks of the Maxwell scheme is that it does not allow describing influence of structure in the inclusion positions on the effective properties. Its results are very dependent on the form of the composite volume examined in the Maxwell scheme (the approach predicts different effective properties of the composite for spherical and non-spherical (ellipsoidal) geometries of this volume [119]).

3.5. Temperature-Dependent Properties

FGMs are also suitable for space applications where high temperature gradients are encountered within a very short time span. Therefore, proper gradation scheme and temperature distributions in FG structures have been active areas of research during last few years in the analysis of such FG structures. In evaluating the behavior of FGMs, Touloukian [120] proposed temperature dependency of material properties *P(T)* as a nonlinear function of temperature by the following expression:

$$P(T) = P_0\left(P_{-1}T^{-1} + 1 + P_1T + P_2T^2 + P_3T^3\right) \tag{6}$$

where P_0, P_{-1}, P_1, P_2 and P_3 are coefficients of temperature T (in K), unique to each constituent materials and determined by experiment [84]. In literature, the multiobjective optimization research related to thermo-mechanical loading of FG plates are carried out [86,87]. They estimated the temperature-dependent effective material properties by either the rule of mixture or the Mori-Tanaka scheme. Similarly, the temperature effect also can be included in the other laws of gradation.

3.6. Finite Element Model

The main purpose behind finite element modeling is to accurately capture the field distribution and use these field data to compute the effective properties. Representative volume element (RVE) model is the most popular homogenization-based multi-scale constitutive method used in the finite element method to investigate the effect of microstructures on mechanical and thermal properties of composites [121]. Numerical study of composite materials involves generation of RVE on which periodic boundary conditions are imposed to predict the overall response of composite material [122–124]. A survey of the existing micromechanical models has been carried out by Raju et al. [125]. They presented that various complex cases incorporating discontinuous fibers, micro-scale voids or pores etc. can be modeled in a super-cell assembly of RVEs with non-periodic random distribution of relevant parameters, based on the geometric complexity of the microstructures. For finite element-based simulation, the case of continuous fiber composite material which is modeled as an RVE with single fiber embedded in the matrix is shown in Figure 6 [125].

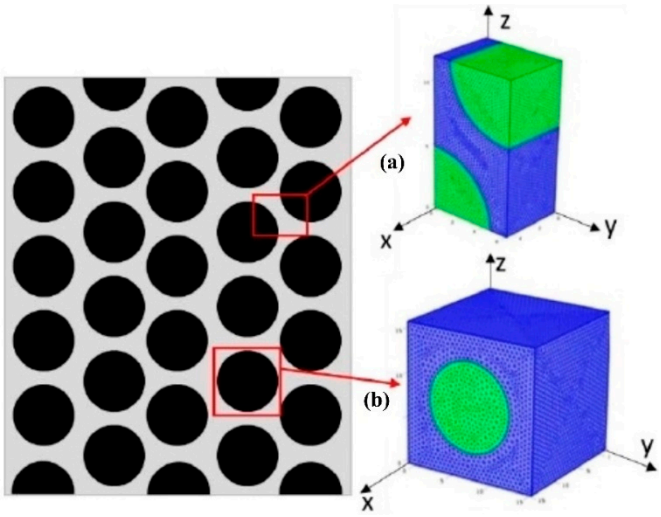

Figure 6. Various fiber packing geometry used in finite element modeling: (**a**) hexagonal packing; and (**b**) square packing. "Reprinted with permission from [125]. Copyright 2018 Elsevier".

Several papers exist in the literature where RVE is analyzed to determine composite moduli. When doing such analysis, there are a few problems that must be carefully considered. The correct boundary conditions need to be applied to the chosen RVE to model different loading situations. When determining the correct boundary conditions, the periodicity and symmetry of the model must be taken into account. A typical RVE can deform in such a way that it retains a right parallelepiped under longitudinal and transverse normal loading.; i.e., plane sections remain plane [126]. Another important issue is the relationship between the actual non-homogeneous stress and strain fields within the RVE and the average stress and strain for the composite. The relationship between the two and the procedure for determining the average quantities are discussed in [121].

3.7. Tamura-Tomota-Ozawa Model

While the classical Hooke's law describes the linear-elastic response of FGMs with the elastic properties evaluated approximately by micromechanics models for conventional composites, determination of the elastic–plastic behavior of FGMs remains a challenging task. The compositional profile and effective mechanical characteristics of FGMs are critical in confirming the manufacturing process and calculating residual stresses and failure strengths. Due to additional material factors, measuring non-linear or elastic-plastic FGMs is more difficult. Unlike elastic FGMs, non-elastic FGMs need identification of not only the Young's modulus but also the yield strength and tangent modulus, which vary spatially. The volume fraction-based model proposed by Tamura et al. [127] is one of the most widely

used models (TTO model). The yield strength of FGMs, as well as Young's modulus and tangent modulus, are calculated using this model. The FGM's compositional profile and the stress-strain transfer parameter that characterizes the effective properties of elastic-plastic FGMs are estimated using an inverse analytical process based on the Kalman filter technique proposed by Nakamura et al. [128]. The TTO model links the uniaxial stress and strain of a two-phase composite (σ, ε) to the average uniaxial stresses and strains of each constituent phase (σ_1, σ_2, ε_1, ε_2) and their volume fractions (V_1, V_2).

$$\sigma = \sigma_1 V_1 + \sigma_2 V_2,\ \varepsilon = \varepsilon_1 V_1 + \varepsilon_2 V_2 \tag{7}$$

TTO model introduces an additional parameter q that indicates the ratio of stress to strain transfer as follows:

$$q = \frac{\sigma_1 - \sigma_2}{|\varepsilon_1 - \varepsilon_2|}, 0 \le q \le \infty. \tag{8}$$

In general, the parameter q is influenced by a number of things (e.g., loading condition, material microstructure and mechanical characteristics of each constituent, etc.). Due to a lack of experimental data, q is presumed constant in most applications even beyond the elastic range [128]. It's worth noting that $q = 0$ denotes that once the metallic elements reach their yield limit, FGMs flow plastically. The effective Young's modulus, E, may be obtained from Equations (6) and (7) [129]:

$$E = \left[V_2 E_2 \left(\frac{q + E_1}{q + E_2}\right) + V_1 E_1\right] \Big/ \left[V_2 \left(\frac{q + E_1}{q + E_2}\right) + V_1\right]. \tag{9}$$

For applications involving plastic deformation of ceramic/metal (brittle/ductile) composites, the TTO model assumes that the composite yields once the metal constituent yields. The effective yield strength, S_y expressed as (Huang et al. [130]):

$$s_y = s_{y2}\left[V_2 + \left(\frac{q + E_2}{q + E_1}\right)\frac{E_1}{E_2} V_1\right] \tag{10}$$

where s_{y2} signifies the metal phase's yield strength. The yield strength of the composite is determined by the yield strength of the metal, the volume fraction of the metal, the Young's moduli of the constituent phases, and the parameter q, as shown in the equation above. Figure 7 shows the yield strength fluctuation of a FGM made up of metal (ductile phase) and ceramic (brittle phase).

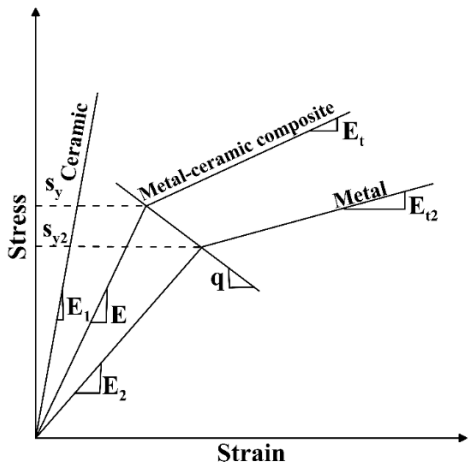

Figure 7. Schematic bilinear stress-strain curve for FGMs. "Reprinted with permission from [131]. Copyright 2020 Elsevier".

For an idealized bilinear model of the metal with a tangent modulus E_{t2} the TTO model predicts that the composite also follows a bilinear response with the tangent modulus E_t given by [129]:

$$E_t = \left[V_2 E_{t2}\left(\frac{q+E_1}{q+E_{t2}}\right) + V_1 E_1\right] \Big/ \left[V_2\left(\frac{q+E_1}{q+E_{t2}}\right) + V_1\right]. \quad (11)$$

The subscripts 1 and 2 in Equations (7)–(11) stand for ceramic and metallic parts, respectively. For many structural metals, the simplistic bilinear model does not capture adequately the variation in strain hardening rate under increased plastic flow [130]. TTO scheme was used by Nikbakht et al. [132] and Komarsofla et al. [133] to acquire the yielding commencement of FG plates and shells, respectively. Recently, TTO model is implemented to describe the elasto-plastic material behavior of FGM disks by Nayak et al. [131]. The above-mentioned references include more thorough information on this model.

4. Representation Techniques

The material properties of FG structures are graded by gradually changing the volume fraction of constituent phases with respect to spatial coordinates in a continuous manner. Therefore, determination of the volume fraction distribution of material constituents of these structures are of prime importance. To represent various types of FGM objects, a variety of theoretical representations, material function derivations, and optimization strategies have been examined. According to model exactness and compactness, Kou and Tan [18] divided heterogeneous object representations into two categories: evaluated and unevaluated models. Evaluated models, such as voxel and volume mesh-based models, can depict heterogeneous material distributions in an inexact and discrete form. Models that have not been evaluated, such as the explicit function model, control feature model, control point model, and implicit function model, do not require extensive spatial decompositions/subdivisions or discretization, and can theoretically provide sufficient fidelity in geometries and material distributions. In terms of representational complexity, another type of heterogeneous object, termed as the composite model, can be identified. The modeling of FGM objects was split into three categories by Zhang et al. [134]: traditional geometrical representation-based FGM modeling, geometry independent FGM object modeling, and a new FGM modeling approach that uses simple material primitives. In the latter category, points, one-dimensional curves (straight lines or splines), and planes are used to build sophisticated material distributions. Recently, Li et al. [135] published a review paper on the developments in heterogeneous object modeling. Their main concentration was on general problems and prevalent solutions along with different design paradigms of the modeling of heterogeneous objects. Each study's disadvantages and advantages were discussed, as well as possible future research projects, in their article. This section aims to review and classify existing FGM object modeling techniques used in studies of material distribution optimization.

4.1. Voxel-Based Models

A heterogeneous object with a collection of voxels is represented by voxel-based models. Each voxel is a tiny cube in space with a specified material distribution (homogeneous or interpolated). Medical data obtained from Computerized Tomography (CT) and Magnetic Resonance Imaging (MRI) scanners are two common examples.

The voxel-based design method, unlike the surface representation method used in most mesh-based CAD applications, can tolerate heterogeneous material qualities in order to modify designs of graded structures. Material distribution in traditional CAD systems is based on pre-existing geometries, but voxel-based approaches can develop material compositions and geometrical coordinates separately. In complicated three-dimensional structures, voxel representation systems can be utilized to embed a wide range of lattice topologies [17]. Because the material composition interrogations are simple, it can be considered a computation-efficient representation [136]. Aremu et al. [137] introduced a

novel voxel-based approach for representing lattice structures with any lattice cell and any exterior geometry. Furthermore, by overlaying a greyscale image onto a pre-designed voxelized domain, voxel-based approaches have been used to build FG structures. It's also worth noting that the rise of voxel design has been strongly linked to the rise of 4D printing. Piezoelectric, electrical, magnetic, and photostrictive materials, as well as transformer hydrogels, have already been used [138].

FGMs are very interested in voxel-based models, but there are still certain obstacles to overcome. The resolution of the voxel has a direct relationship with the model's accuracy. Huge storage spaces are usually required to obtain an accurate heterogeneous model. A database for material distribution should be established ahead of time, which will necessitate considerable testing. Designers must master both the geometrical modeling process and the materials science features of the pieces that will be printed (e.g., material compositions, structures, properties, and performance).

4.2. Volume-Mesh Models

Volume mesh-based models are similar to voxel-based models. The only difference is that they use a collection of polyhedrons instead of spatial grids to represent three-dimensional models [139]. The mesh nodal vertices are similarly defined as voxels; however, the material distributions at other locations inside a polyhedron are not explicitly evaluated and preserved in datasets; instead, they are represented by a function through interpolations. This representation alleviates the huge storage problem in the voxel model and is more compact in data structures. In addition, volume mesh-based representations are able to represent complex/highly heterogeneous material distributions [140]. In a very recent paper by Saini et al. [141], heat conduction of heterogeneous materials with varying volume fraction, shape and size of fillers was evaluated using adaptive mesh generation method.

Despite these advantages, mesh-based representations also suffer from a few limitations. As reported by Sharma and Gurumoorthy [142], evaluated models use a mesh or voxel representation to approximate the geometry. It is difficult to prescribe the material distribution using geometric form features (like holes), or user-defined material reference entities, as the geometric information about the features is lost after discretization. Furthermore, the depiction of material composition using these models is dependent on the mesh resolution or voxels, which may or may not conform to the material distribution, resulting in discretization inaccuracy. In addition, any change in material function would lead to re-discretization of the whole geometry to reapproximate the new material distribution.

4.3. Explicit Function-Based Models

Analytical functional representations apply explicit functions to manipulate the material composition at each point inside the FGM model [143]. One advantage of the explicit functional models is that the material interrogation can be extremely fast and efficient, because evaluations of analytic functions are rather trivial for modern computers. In addition, explicit functional models are simple to comprehend and formulate. Linear, exponential, parabolic and power function based material distributions have been widely used in modeling heterogeneous material distributions [18]. For instance, Srividhya et al. [104] modeled a unidirectional FGM plate with power-law functions. This approach is very easy to use and greatly simplifies the optimization step (because only a few parameters need to be optimized). Very similar equations were used by Arslan et al. [64].

The modeled material distributions are usually of simple shapes when using explicit functions (e.g., unidirectional or one-dimensional material gradations). For objects with complex heterogeneities, it is usually difficult to model the entire material distributions with an explicit, analytic function. Another drawback of this model is related to its dependence of specific coordinate systems and certain geometrical transformations.

4.4. Control Point-Based Models

Traditional modeling methods for heterogeneous structures, such as boundary representation (B-rep) and Constructive Solid Geometry (CSG), are not the best. This is because they do not allow representation of the inside of the object precisely. Control point-based models can be regarded as direct extension of parametric curves, surfaces and volumes, with additional material information assigned to each of the control points. The detailed implementation of B-splines basis function to obtain the volume fraction distribution of FGM is provided by Nayak and Armani [144]. In order to reduce the mass and deflection of FGS plates subjected to mechanical stresses, Ashjari and Khoshravan [145] provided an optimization method based on NSGA-II with the stress field as the constraint. A piecewise cubic interpolation function was used to calculate the distribution of the material volume fraction after it had been defined at some control points. The design factors for this study were these control points, the volume fraction distribution, and the thickness of the face sheets.

Based on the stochastic Voronoi diagram and B-spline representation, Kou et al. [146] proposed a novel digital model to design generic porous structures with graded porosities and irregular pore distributions. They proposed a new method to model the microstructures with FGM distributions. As the extension of [146], this approach does not require expensive imaging equipment during the design process, and digital models can be constructed at interactive or quasi-interactive rate.

With the advent of isogeometric analysis (IGA), the modeling of spline solids became an important topic. IGA was first developed by Hughes et al. [147] towards the integration of CAD and FEA into a single model. Geometric domains in the CAD environment and FEA solutions are uniformly modeled and estimated in this technique, which is based on B-splines or NURBS functions. In a paper by Do et al. [148], IGA was used to integrate CAD and FEA to analyze the behavior of FG plates. Yavari and Abolbashari [149] analyzed the thermoelastic waves propagation in non-uniform rational B-spline rods under quadratic thermal shock loading using IGA approach. A recent paper [150] presents computational optimization for porosity-dependent isogeometric analysis of FG sandwich nanoplates. The ceramic volume fraction distribution was approximated by using the multi-patch B-spline basis functions through the thickness direction.

Control point-based models are compact in both geometry and material representations. In addition, this model can effectively represent complex (two- or three-dimensional dependent) material distributions. The limitation of this model is that it relies heavily on spatial parameterizations and for arbitrary three-dimensional objects such parameterizations remain a rather non-trivial task [134].

4.5. Implicit Function-Based Models

Implicit function based models use the functional representation (F-Rep) as the basic model for both the point set geometry and the material distribution [151]. The F-rep for the material attribute can be symbolically described as:

$$G = \left\{ X = (x, y, z) \in E^3 | f(X) \geq 0 \right\} \tag{12}$$

where $F : E^3 \rightarrow R^N$ is a material distribution function defined in the three-dimensional Euclidean space [134]. In this representation scheme, the geometry of the object is described in the form of functions $f(x, y, z) \geq 0$. The surface/boundary of the object would be the vertices satisfying $f(x, y, z) = 0$, and the interior points are expressed as $f(x, y, z) > 0$.

The implicit functional models are also highly efficient, since the point membership classification (PMC) is based on evaluation of real-valued functions, and the material composition can be also easily interrogated using a lookup table (in the case of multi-material objects) or evaluated directly from explicit functions. More importantly, F-Rep facilitates constructive modeling of complex objects from simple primitives in a similar fashion as the classical CSG representation [151].

4.6. Composite Models

When modeling generic objects with complex material distributions, two or more different types of material distributions might occur in different portions of the same object. Hybrid homogeneous, unidirectional, or tri-variate FGM distributions, for example, may arise in different parts of the same component. In theory, a composite model is a collection of sub-objects, each of which belongs to a specific material domain [152]. There are various representation approaches for spatial decompositions, for example, assembly representation and cellular representation [18].

The assembly representation partitions the objects into several parts through direct decomposition or constructive approach. While in cellular decomposition representation, the geometry might be expressed with non-manifold boundaries due to the material distribution. By introducing the concepts of co-boundaries, the cellular model has better data storage efficiency than the assembly model [18]. Figure 8a shows an object with complex material distributions, and Figure 8b,c are the assembly representation and cellular model, respectively. Recently, the cellular representation approach was successfully applied in bio-modeling of heterogeneous bones [153].

Hybrid composite models can describe structures with more intricate material distributions by incorporating both assembly and cellular models, and the strengths of each representation can be fully exploited, as demonstrated in Figure 8. In a manner similar to the volume mesh-based representation, a hybrid cellular functional model was proposed to represent complex heterogeneous objects [154]. The hybrid composite models utilize different types of material representations in the same composite model. Therefore, the representational capacity is generally large and can be used to model a variety of heterogeneous objects. Other properties of hybrid composite models are mostly case-specific: the compactness, efficiency and accuracy are all dependent on the characteristics of the involved component models [135].

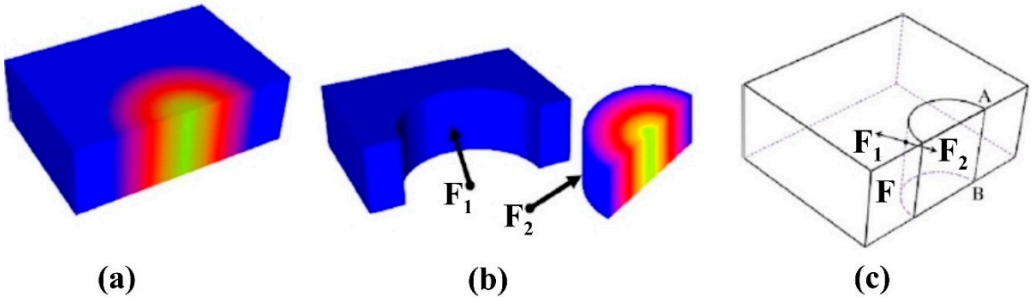

Figure 8. An example of (**a**) an object with complex material distribution; (**b**) the assembly model of the object; and (**c**) the cellular model of the object. "Reprinted with permission from [18]. Copyright 2007 Elsevier".

4.7. Material Primitive-Based Models

As discussed in previous sections, a number of representation schemes are available for FGM representation. The material information is represented either by extending existing geometric representation or based on the coordinate systems. For conventional geometric representation-based FGM modeling, the material distribution is confined by the geometric structure of the objects. This limits the freedom of modeling irregular and compound material variations. For geometry-independent FGM object modeling, the material configuration has a strong dependence on the coordinate system. From the users' perspective, this may not be favorable in capturing their intentions. Numerous new material primitive-based frameworks have been explored in the literature for a systematic and generic modeling of FGM objects.

The material convolution surfaces-based approach is presented by Gupta and Tandon [155] for modeling FGM with material primitives (Figure 9). Various material distributions can be efficiently modeled with the material primitives. By adjusting the char-

acteristics of the convolution surface-based material primitives, the material distribution in the object can be improvised correspondingly. Although the material convolution surface-based scheme is potent for modeling FGM objects, it has the glitches of high data redundancy resulting from unnecessary memory occupation. Besides, it faces the data inconsistency between material and geometry models near boundaries, particularly in the case of spline primitives.

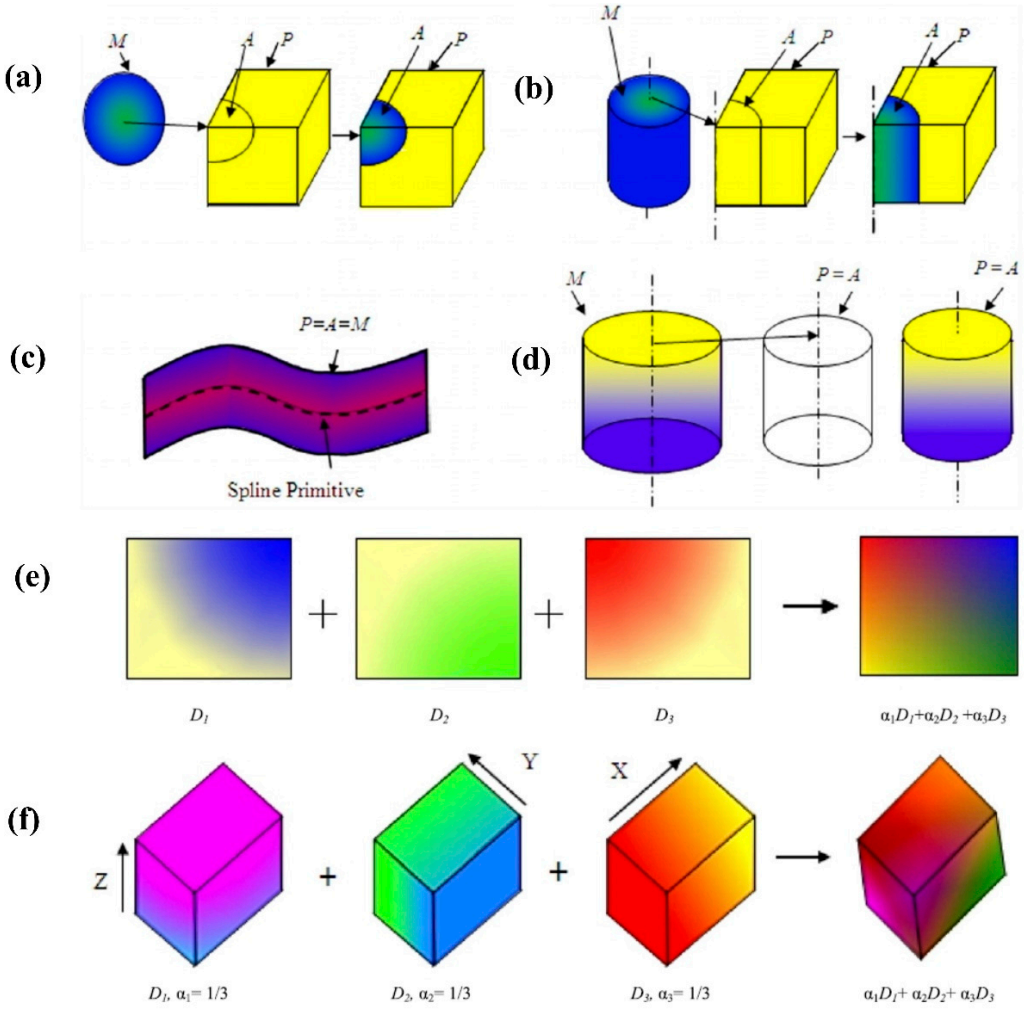

Figure 9. Material modeling with convolution surface-based material primitives: (**a**) point; (**b**) straight line; (**c**) spline; (**d**) plane; (**e**) two-dimensional material distribution in an object obtained by merging three one-dimensional material distributions; and (**f**) three-dimensional material distribution in an object. "Reprinted with permission from [155]. Copyright 2015 Elsevier".

To model complex heterogeneous object with complex geometries efficiently, Sharma and Gurumoorthy [142] proposed a hybrid representation to capture arbitrary material distribution using mixed-dimensional entities and represent it even when these entities are not part of the shape parameters or topological entities of the solid model of the part. They used medial axis transform (MAT) to define the domain of effect of each material reference entity, where the material distribution can be intuitively prescribed, starting from the material reference entity and terminating at the medial axis segment bounding the corresponding domain. Recently, Sharma and Gurumoorthy [156] implemented an iso-material contour representation to generate the process plan for additive manufacturing given a smooth representation of heterogeneous object model. By interpolating material composition along the lines linking the places on the source to the appropriate target entities, iso-material contours are recovered between source and target reference entities.

The hybrid representation also allows the construction of such contours on demand at any specified resolution/accuracy. In addition, this method possesses all the advantages of hybrid representation that include adaptive discretion based on the material distribution, efficient material interrogation for numerical analysis and manufacturing planning.

4.8. Comparison

The above classifications and evaluations are aimed at providing a rough idea of different models and their characteristics. Table 1 outlines the above discussed models and their properties.

Table 1. Comparisons of different heterogeneous object models. Material capability A: multiple and B: multiple with gradient functions. ☆ ☆ ☆ ☆: very good, ☆ ☆ ☆: good, ☆ ☆: average, ☆: poor, /: uncertain or case-specific.

Representations	Material Capability	Representational Capacity	Accuracy or Exactness	Compactness Overhead and Efficiency
Voxel model	A	☆ ☆ ☆ ☆	☆	☆ ☆ ☆ ☆
Volume mesh model	A	☆ ☆ ☆ ☆	☆	☆ ☆ ☆
Explicit function model	B	☆ ☆	☆ ☆ ☆ ☆	☆ ☆ ☆ ☆
Control point based model	B	☆ ☆ ☆	☆ ☆ ☆ ☆	☆ ☆ ☆
Implicit function model	B	☆ ☆ ☆	☆ ☆ ☆ ☆	☆ ☆ ☆ ☆
Hybrid composite model	B	☆ ☆ ☆ ☆	/	/

5. Finite Element Analysis Approaches

The complexity and cost associated with the manufacture and testing of FG specimens has intensified the use of numerical tools to analyze their mechanical response. Although a variety of numerical techniques have been used, including mesh-free methods and enriched formulations, the finite element method is by far the most popular approach [157]. The finite element method as an efficient numerical tool has been used for the simulation of FGMs due to its ability to handle complex geometry, loading, material and boundary conditions. Since there is currently no commercial software capable of analyzing FGMs, researchers have either modified existing software, or developed their own codes. The first option enables solving problems with complex geometries and physics, and implementing complex material composition distributions. On the other hand, indigenously-developed codes have more flexibility in implanting different homogenization approaches and representation techniques, but it is not feasible to do multi-physics analysis of three-dimensional parts using them. Here, we have first explained FEA for the optimization of FGMs using commercial software and then provide a few examples of indigenously-developed codes.

5.1. Commercial Software

Zhang et al. [97] modeled FG parts in Abaqus using a USDFLD subroutine. This subroutine allows users to define material properties as functions of field variables including location. Abaqus was used by Bahraminasab et al. [85] to improve the femoral component of FGM knee implants. The goal of this optimization study was to minimize the problem of knee implants loosening. Multi-layered configurations were used to model the FG structure and each layer was assumed to behave as a homogeneous isotropic linearly elastic material, except for ultrahigh molecular weight polyethylene, which was modeled as an elastic-plastic material. The topology optimization was carried out by Ramírez-Gil et al. [158] for cylindrical steel plates in ANSYS APDL. The optimization problem required an FEA at each iteration and used the equivalent static load method to convert the dynamic loads to static loads. For the three-dimensional optimal design of FGMs, Ghazanfari [159] developed a Fortran code written using USDFLD function to enable implementation of FGM in Abaqus. In a paper by Zhou et al. [160], finite-element (FE) modeling was used to investigate the thermodynamic behavior of the Thermal Protection System (TPS) utilizing bolted joints made up of porous $ZrO_2/(ZrO_2 + Ni)$ FGMs. The transient response of the

porous $ZrO_2/(ZrO_2 + Ni)$ functionally graded bolted joint was obtained by thermodynamic simulations. The effects of the preload on the thermomechanical behavior and service reliability of the bolted joint were numerically analyzed in detail by ABAQUS codes. In a subsequent paper, Zhou et al. [161] investigated the load distribution in threads of the TPS utilizing bolted joints made up of porous $ZrO_2/(ZrO_2 + Ni)$ FGMs by ABAQUS codes.

A software package, MicroFEA 1.0, for finite element analysis of FGMs has recently been developed by Medeiros and Parente [162]. The software package can be used for the material optimization of heterogeneous materials. The package included MATLAB scripts and Fortran subroutines for use with Abaqus for Finite Element Analysis (FEA). At the integration point level, the Abaqus user-material subroutines (UMATs) were built to operate with heterogeneous materials. In addition to UMAT, the analysis of FGM structures subjected to thermomechanical loading required the use of UTEMP subroutines to define the temperature field. More recently, Nayak and Armani [144] analyzed the optimal distribution of FG parts in ANSYS APDL using a USERFLD subroutine. The USERFLD function in ANSYS provides users with the capability of defining field variables as functions of time or other quantities. Node-based initial state helps initialize the user-defined field variables that are then used by the TB database to evaluate the material properties at an integration point.

FEA has been frequently utilized to improve the strength-to-weight ratio of FG scaffolds by optimizing the distribution of graded cellular lattice structures [163–165]. Kladovasilakis et al. [166] recently published a paper on orthopedic hip implant with FG bioinspired lattice structures through FEA under in vivo loading. ANSYS was used for the finite element analysis and in particular, the static structural module was used to simulate the quasi-static loading.

COMSOL Multiphysics can also define the material properties of FGM through analytic functions to analyze the mechanical behavior of FGM structures. Based on the first order shear deformation theory (FSDT), Kolahi et al. [167] developed an analytical framework for mechanical study of thick, shrink-fitted FG cylinders (FSDT). Additionally, they used COMSOL Multiphysics to perform a finite element simulation, which has the benefit of defining material properties as analytical functions. Sharma et al. [168] investigated the modal analysis of an axially functionally graded material beam under hygrothermal effect. The material constants of the beam were supposed to be graded smoothly along the axial direction under both power law and sigmoid law distribution. COMSOL Multiphysics (version 5.2) package was used to find the Eigen frequencies of the beam. Meshless weighted least-square (MWLS) method was extended by Zhou et al. [169] to solve the thermoelastic problems of FGM beam with interior heat source, and verified by comparing results with the solution computed from the commercial COMSOL Multiphysics software.

5.2. Indigenously-Developed Codes

When developing finite element codes for material optimization of FG structures, it is important to seek a balance between accuracy and computational efficiency. The finite element method based on Vlasov's thin-walled theory was developed by researchers [170]. They developed finite element formulation for geometric and material optimization of thin-walled FG beams for buckling problems. Hussein and Mulani [171] optimized the volume fraction of thin plates subjected to buckling constraints using classical plate theory and finite element approach.

The use of finite element models based on appropriated shear deformation theories is important for the design optimization of FG plate structures [87,172]. The FSDT is the most popular one because it provides both adequate accuracy and efficiency. Compared to the first-order shear deformation theory, the higher-order shear deformation theories (HSDTs) offer a slight improvement in accuracy but at the expense of an increase in computation effort. An FEM based on HSDT was applied to develop a discrete model for the structural and sensitivity analyses allowing for the material distribution and sizing optimization of FGM structures [173]. Correia et al. [174] considered the material optimization of FG

plates subjected to thermomechanical loading using finite element models based on appropriated shear deformation theories. A nine-nodes Lagrangian finite element plate model based on HSDT, considering the transverse shear and transverse normal deformations and accounting for the temperature dependency of the material properties, was used in the work.

5.3. FEM Integrated with CAD

As mentioned in Section 4.4, researchers developed IGA towards the integration of CAD and FEA into a single model. The IGA method has several advantages over conventional FEA such as being capable of refining mesh via re-indexing parametric space with no interaction with CAD system. Furthermore, even at the coarsest discretization level, the precise geometric is preserved. Furthermore, the method is effective in lowering the number of degrees of freedom (DOFs) for higher-order elements. C^1-continuity of the generalized displacement field is required for HSDTs, which leads to the second-order derivative of the stiffness formulation. This makes standard finite element formulations difficult. To address this flaw, extra C^0 continuous elements were added, or a Hermite interpolation function with the C^1-continuity was added for the precise approximation of transverse displacements. These methods can generate additional unknown variables, such as deflection derivatives, resulting in high computing expenses. While the displacement fields in the HSDT were created using NURBS basis functions, which may provide higher order continuity and hence easily meet the requirement of C^1 transverse displacement continuity. This is a benefit compared to the finite element method. Furthermore, when employing the same high-order elements, the IGA requires a substantially less number of DOFs than the traditional FEM.

Taheri et al. [175] developed a methodology in the framework of IGA for optimization of thermo-elastic material distribution of functionally graded structures. In this approach, variations of the material constituents' volume fractions were constructed by imaginary NURBS surfaces in a fully isogeometric formulation using the same basis functions employed for construction of the geometry and approximation of the solution. The modeling and optimization of the ceramic volume fraction distribution of FG plates in the framework of the IGA was conducted in a paper by Lieu and Lee [86]. Optimal material distributions of tri-directional FG plates under free vibration or compression in various volume fraction constraints were found by an isogeometric multi-mesh design (IMD) technique in [148].

6. Optimization Algorithms

The optimum response of a part to an actual environment is the main objective in the design of FGMs. Many strategies have been proposed for the optimization of material distribution in FGMs, thus far. Sequential quadratic programming (SQP) method [41] has received considerable attention in material distribution optimization of FG structures (e.g., [77,90,171,175–177]). Gradient-based approaches, including SQP, rapidly converge to optimal solution, but are often trapped at local optimal solutions. Furthermore, sensitivity analysis of the fitness and constraint functions are always required, and performing such analyses is both difficult and expensive. To avoid these shortcomings, derivative-free algorithms, also known as metaheuristic approaches, such as differential evolution (DE) [178], particle swarm optimization (PSO) [179], genetic algorithm (GA) [57], simulated annealing (SA) [180], and symbiotic organism search (SOS) [181] have been developed. Since stochastic searching techniques are employed to randomly choose potential candidates in a given space, sensitivity analyses are avoided. Consequently, a global optimal solution can be obtained without requiring a rigorous mathematical analysis. Their disadvantage is the high computational cost, especially for optimization problems with many design variables.

Among derivative-free methods, DE is a simple population-based stochastic algorithm that may be initialized by sampling the objective function at multiple randomly-chosen initial points. DE has shown its effectiveness in numerous engineering applications [182]. Tsiatas and Charalampakis [183] utilized the DE algorithm for optimizing the material

distribution of axially FG beams and arches, which led to the maximum first fundamental frequency of these structures. More recently, Truong et al. [184] introduced a novel and effective approach as an integration of artificial neural network (ANN) into DE to the material distribution optimization of bidirectional functionally graded (BFG) beams under free vibrations.

Another derivative-free optimization approach is PSO, which was originally proposed and developed by Kennedy and Eberhart [185]. PSO has several advantages, including excellent robustness, simple implementation, and well-adapted handling of non-linear non-convex design spaces with discontinuities. These advantages make it ideal for use in many applications. It can also easily handle continuous, discrete, and integer variable types. PSO is more efficient, requiring fewer number of function evaluations compared to other robust design optimization methods, while achieving better or the same quality of results [186–188]. Recently, PSO has been proved to be useful on material distribution optimization of FGM structures [144,188,189].

Genetic algorithm is a non-gradient stochastic optimization algorithm, which has been widely used in finding global optimality. The application of genetic algorithms to solving composite optimization problems is increasing, especially over the last few years. A relatively recent review of GA use in composite structures optimization was published by Wang and Sobey [190]. GAs are inherently easy to parallelize since the fitness evaluation for each member of the current population can be evaluated simultaneously in parallel, thus reducing the optimization time [41]. With regard to the optimization of material distribution of FG structures involving GA, the following publications can be mentioned: [41,170,191]. Nikbakht et al. [192] published a review paper on optimization of FG structures. The most common optimization design variable in the evaluated works is the material distribution pattern, according to this review, which addressed numerous types of structures made from FGM. In addition, it was noted that the methodologies based on GA and PSO are, so far, the most frequently-used algorithms.

The SOS algorithm is simple and effective, and it was inspired by natural symbiotic relationships between species. Moreover, it requires no specific algorithm parameters. The implementation of SOS is seen in large number of researches [193–196]. Nevertheless, a noticeable restriction of SOS is computational cost, comparable to other derivative-free algorithms. Therefore, SOS is modified by the authors [197] to decrease computational cost but still ensure solution precision. The new algorithm is called modified symbiotic organisms search (mSOS). The effectiveness and robustness of mSOS have been demonstrated through pin-jointed structures and unidirectional FG plates in terms of convergence speed and solution accuracy [197]. The application of mSOS for optimizing the material distribution of the FG structures has been addressed in the literature [148,198].

Yang [199–201] resented another optimization strategy, the so-called firefly algorithm, as a generalization of the PSO, SA, and DE algorithms (FA). This algorithm combines the benefits of the previous three and can be used in a variety of situations [202]. Both techniques' convergence rate and solution correctness, however, still need to be improved. The adaptive hybrid evolutionary firefly algorithm was developed by Lieu et al. [203] as a hybridization of the DE method and the FA method (AHEFA). In comparison to many other approaches, this approach has been successfully applied to shape and size optimization problems of truss structures with multiple frequency constraints, demonstrating its effectiveness and robustness in improving the convergence speed and accuracy of the obtained optimal solution. Recently, it has been applied to material distribution optimization of multidirectional FG structures [86,150,204,205].

To find the direction vector of design variables for volume-fraction optimization, a sensitivity analysis of the related objective function should be done. The direct analytical method, however, becomes unavailable in almost all circumstances due to the intricate and implicit relationships of temperature and stress fields to the volume fraction. As a result, various available and efficient approaches are used, such as the finite difference method (FDM), semi-analytic method, and objective function approximation method using

a neural network [40]. Aside from material property estimation and sensitivity analysis, the approximation of the volume-fraction field should be considered since it affects the volume-fraction distribution's flexibility and inherent continuity, as well as the number of design variables. As a remedy for suppressing the CPU time increase, the approximation of the design space is widely being adopted by the employment of artificial neural network (ANN) [206]. Accordingly, the ANN significantly reduces the computational cost, yet still achieving a high-quality global solution. There have been several works (e.g., [148,184,198]) reported to optimize the material distribution of FGMs using ANN.

7. Most Advanced Design Methods

Most research papers in this area are proposing a new design method. Some of these methods are capable of handling only simple problems (e.g., one-dimensional material distribution with one-dimensional geometry and simple loads), while some can tackle more sophisticated problems (e.g., three-dimensional material distribution with three-dimensional geometry and multiple types of loads). Thus, the powerfulness of a method could be judged based on its capabilities. In this section, the most advanced design methods are identified, explained, and analyzed in terms of their advantages and disadvantages.

As described in Section 5.3, IGA was used in some studies as an alternative to standard FEM because it requires far fewer DOFs with same high-order elements. In this method, most common B-splines/NURBS functions in the CAD environment are utilized to exactly model geometric domains as well as approximate unknown solution fields in the analysis. These functions can naturally fulfill any desired high-order derivatives and continuity by choosing a suitable order corresponding to its knot vector. Due to the above-mentioned properties, IGA has been broadly applied to various problems, especially for material distribution optimization of FG plates in recent years.

As shown in Figure 10, 2D-FG plates have a volume fraction of each constituent material that varies in both directions through the plane. This type of FGM is most commonly used in cutout designs, where the two-dimensional variety of materials results in improved stress distribution or high temperature resistance. The multi-directional material dispersion around these holes is responsible for these notable characteristics. Lieu and Lee [86] used Greville abscissae to estimate the volume percentage of ceramic in a FG plate at certain grid points along the thickness and a B-spline basis function to approximate material distribution along the thickness. Temperature dependence was postulated for the basic materials. The plates were exposed to thermomechanical loads, and IGA and AHEFA were used to identify the optimal material distribution that resulted in the lowest compliance. Their algorithm produced more precise findings and improved the convergence speed. In addition, AHEFA is very promising in providing an effective optimization tool for various real problems. Subsequently, to maximize the fundamental frequency of multi-directional FG plates, Lieu and Lee [204] used AHEFA in the context of isogeometric multi-mesh design (IMD). The material inhomogeneity as well as the thickness variation profile were used as design variables in their investigation of several plates with constant and varying thicknesses.

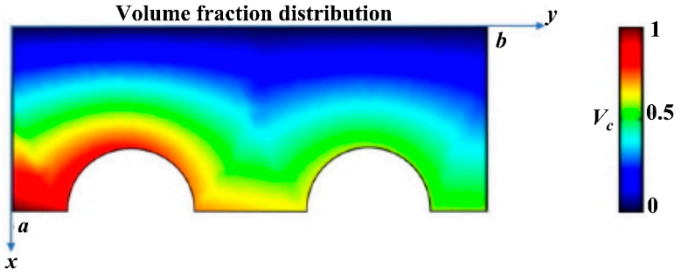

Figure 10. In-plane volume fraction distribution in a 2D-FG plate. "Reprinted with permission from [179]. Copyright 2012 Elsevier".

Do et al. [198] used two optimization tests on two-dimensional FG plates to show that the mSOS approach outperforms the DE and SOS methods. By getting the optimal material gradation through these structures, the fundamental frequency and buckling load were maximized. These researchers also demonstrated that integrating mSOS with the Deep Neural Network (DNN) approach considerably reduced processing time and outperformed mSOS in the context of isogeometric analysis. In a subsequent paper, Do et al. [148] optimized the material distribution of tri-directional FG plates using DNN and IMD approach. They used DNN to supplant FEA to reduce computational cost and to predict directly the behavior of multi-directional FG plates from those material distributions. Furthermore, the researchers were able to construct NURBS surfaces using the aforementioned method, resulting in significantly cheaper computational costs during the optimization process.

Nayak and Armani [144] recently suggested a new methodology for optimizing material distribution for three-dimensional FG parts in order to take advantage of the capabilities of AM techniques in manufacturing FGMs with complicated material distributions. To establish a strong and versatile "foundation" for optimal design of FG three-dimensional parts, appropriate material models, FEA technique, and optimization algorithm were selected, applied, updated, and combined. Furthermore, the proposed method is more effective at dealing with complex material composition constraints and complex geometries.

Going beyond structural mechanics, design of multi-scale structures involving other physics and even multi-physics is another important venue to explore. Some of the works along this direction have been mentioned in previous sections when specific multi-scale approaches were introduced. Porous materials that enable light-weight designs with superior performance are now widely used in a variety of industries. Engineers have been inspired by natural porous bones and have succeeded in further altering the properties of porous materials by establishing the FG porosity concept and optimizing the porosity pattern in these materials. For instance, Das and Sutradhar [92] presented a multi-physics topology optimization of FG controllable porous structures to optimize heat-dissipating structures considering structural and thermal performance. The control over porous geometry (functional gradation of porosity, pore size, and sensitivity-based porosity control) to design FG porous structures may satisfy multi-functional requirements in many engineering applications.

Recent years have seen a rapid development in topology optimization approaches for designing multi-scale structures involving improved stiffness, different modes of heat transfer (e.g., convection) and fluid flow can provide promising optimized porous structures with enhanced multi-physics performance for thermal management of power electronics package, electric vehicle battery cooling, heat transfer in extreme environments, energy absorption devices, and nuclear reactors. Jamshidi and Arghavani [207] used a multi-objective optimization approach based on NSGA-II to maximize the porosity distribution of 2-D FG porous beams. An FG porous beam with a rectangular cross-section of unit width, thickness h and length l, is shown in Figure 11a and a quarter of the beam as optimization domain as shown in Figure 11b. The goal was to maximize the buckling load while minimizing the weight. Several examples with various symmetrical clamped and hinged border conditions were presented by the researchers. They reported that in most of the ideal designs, porosity was concentrated in the centre of the beams rather than the outer corners. Furthermore, boundary conditions were discovered to have an impact on the final outcomes and the best porosity distribution. Banh et al. [208] presented an effective non–homogeneous multi-material topology optimization paradigm for FG structures, considering both cracked and non-cracked cases. They employed an enrichment finite element concept known as the extended finite element method (X-FEM) to analyze strong discontinuity states critical mechanical behavior. In addition, a block Gauss–Seidel-based alternating active-phase algorithm is utilized to convert a multiphase topology optimization problem subjected to multiple constraints to many binary phase topology optimization sub-problems with only one constraint. The comparison for most advanced

design methods of FGMs of few published research works are listed in Table 2, briefly and specifically.

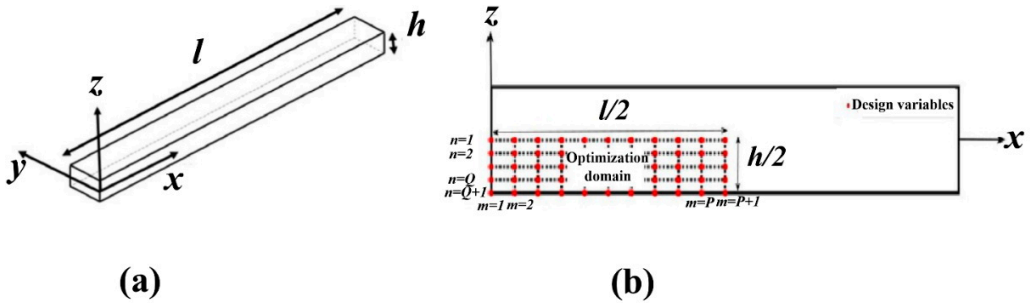

Figure 11. Schematic of (**a**) FG porous beam and (**b**) optimization domain in the FG porous beam. "Reprinted with permission from [207]. Copyright 2017 Elsevier".

Table 2. Comparison of published articles on advanced design methods of FGMs.

	Handle Complex Geometry	Handle Complex Material Distribution	1D,2D,3D Material Distribution	Handle Multi-Physics	Optimizing Geometry as Well	Realistic Material Model	Manufacturing Constraints	Convergence Speed
Lieu and Lee [204]	✓	✓	3D	✓	✓	✓	✗	Fast
Do. et al. [148]	✓	✓	3D	✓	✗	✓	✗	Mediocre
Nayak and Armani [144]	✓	✓	3D	✓	✗	✓	✓	Slow
Das and Sutradhar [92]	✓	✗	1D	✓	✓	✗	✗	Mediocre
Jamshidi and Arghavani [207]	✓	✗	2D	✓	✗	✗	✗	Fast
Banh et al. [208]	✓	✓	1D	✗	✓	✗	✗	Fast

8. Manufacturing Techniques

Manufacturing procedures are important in producing the desired compositional and microstructural distribution, as well as the characteristics of FGMs. Several conventional manufacturing techniques are capable of manufacturing FGMs [8], but they have apparent limitations as they can only create simple FG objects with simple gradients [134]. The advent of additive manufacturing processes has opened up new possibilities for designers and engineers to produce FGMs. In addition, AM offers the benefit of enabling for flexible designs that can be optimized for specific geometrical requirements or applications where complex procedures or geometries are too time-consuming, expensive, or impossible to manufacture using traditional methods. AM can use three types of materials: (a) single-phase materials with gradual density variations (e.g., cellular structures); (b) two or multi-phase materials with gradual material composition variations; and (c) a mixture of these (i.e., with gradual density and material composition variations). Many AM processes can produce multi-material and FG structures [14,15,209], but only a few AM processes are able to build FGMs with complex distribution of material composition. Here, we focus on providing a brief explanation of these AM techniques.

8.1. Direct Energy Deposition

By melting metallic wires or powders with a focused electron or laser beam, direct energy deposition (DED) technologies can repair, reinforce, or clad components. Direct laser metal deposition (DLMD) is a typical DED process that is separated into two groups based on the materials used: wire arc additive manufacturing (WAAM) and laser metal deposition (LMD). The WAAM technique (Figure 12a) can use wires derived from different metals such as pure titanium and 1080 pure aluminum to manufacture components with a chemical composition gradient by adjusting the individual wire feeding speed [210]. Similarly, by altering the volume of particles supplied into a melt pool under a moving laser, a metallic graded object can be created by LMD (Figure 12b) [211]. Because DED procedures rely on fusion, the formation of intermetallic phases in the gradient zone might cause undesired characteristics during solidification. Carroll et al. [212] looked at the characterization and thermodynamic modeling of FG 304L stainless steel/Inconel 625 to see if it was feasible. In the graded zone, there were approximately 24 layers, and the volumetric concentration of each powder changed by 1 vol percent (Figure 13a). The same deposition approach was used by Qian et al. [213] to alter the mass fractions in an airplane beam (Figure 13b). The highly loaded exterior of the beam was made of high strength TA15 (Ti-6.5Al-2Zr-1Mo-1 V), while the less loaded interior was made of high ductility TA2 (Grade 3 CP-Ti).

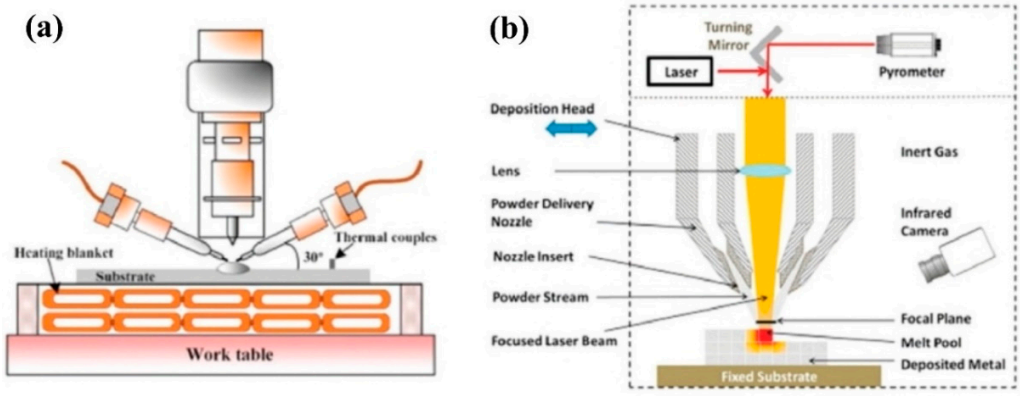

Figure 12. DLMD methods:(**a**) double-wire feeding process. "Reprinted with permission from [210]. Copyright 2018 Elsevier."; and (**b**) metallic powder process. "Reprinted with permission from [211]. Copyright 2015 Elsevier".

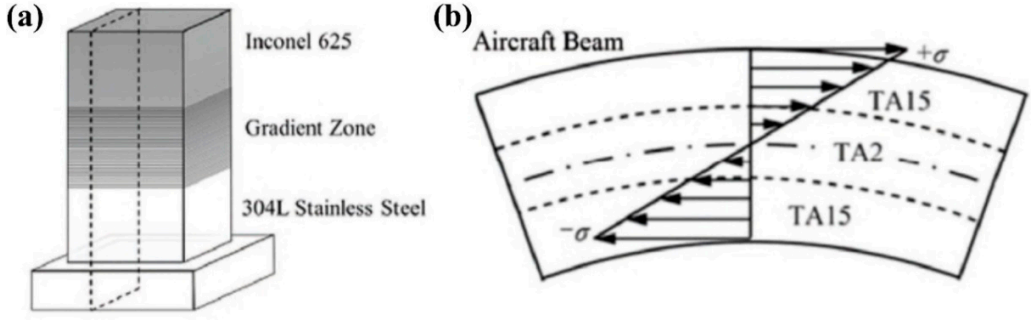

Figure 13. (**a**) Schematic of a graded alloy specimen. "Reprinted with permission from [212]. Copyright 2016 Elsevier."; and (**b**) schematic of an FG structure in an aircraft beam. "Reprinted with permission from [213]. Copyright 2014 Elsevier".

8.2. Material Extrusion

Material extrusion methods use multiple extruders, each extruding a paste or filament at a different flowrate, to produce FGM. Extrusion-based additive manufacturing of FGM (e.g., ceramic on-demand extrusion [214,215]) involves computer-control of flows

of each material, the mixing of these materials, and the extrusion of the mixed material to fabricate a three-dimensional part layer-by-layer. Two or more materials are extruded simultaneously by a multi-extruder mechanism. During the component fabrication process, continuous control of the material compositions and gradients can be achieved by planning (considering time delay) and controlling the relative flowrates of the various materials.

Bakarich et al. [216] succeeded in fabricating an artificial tendon-muscle-tendon system with spatially linear changing colors using soft hydrogel and rigid UV-curable acrylate urethanes. The advancement of current equipment and technology has also enabled the production of nonlinear gradient materials. Ren et al. [217] created a three-axis motion gantry, an active mixing device, and a digital material feeding mechanism for a 3D printer. Mathematical functions were employed to represent the graded distribution of material attributes during the printing process. The nano-sized Al_2O_3 particles were then digitally fed into the printer to manufacture one-, two-, and three-dimensional graded objects using gray-scale representation and regulating code generation.

Material extrusion processes are lower-cost AM methods that use less expensive materials and pose no risk of toxic gases and chemical contamination. However, after printing, the surface is rough and may require additional steps. Additionally, its limited printing precision makes it difficult to generate precise gradients.

8.3. Material Jetting

UV radiation is used to cure and smooth objects created by applying a liquid photopolymer in material jetting process. Several inject heads can be used in this procedure to deposit multiple materials at once to manufacture FGMs with different graded properties including stiffness, transparency and color [218]. As shown in Figure 14a, an array of print-heads moves along the X and Y directions and spray photopolymerizable material onto a table. The roller smoothens the surface of the sprayed materials, and the UV lamp cures the material. After the jet printing and curing of one layer is completed, the table drops by the thickness with a high degree of accuracy. These steps are repeated until the entire part is built. In Figure 14b, TiC/steel FGMs processed by material jetting technique is shown [219]. To create circular and rectangular graded zones, Salcedo et al. [220] employed Tango Black+ (TB+, a rubber-based substance) and Vero White (VW+, an ABS-based material). With very small changes, the strain patterns predicted by FEA matched those obtained from the experimental tensile test. Although commercial software such as Grab CAD is available for material jetting to achieve some basic physical property variations (e.g., graded color, transparency, and stiffness), there are only a few materials that can be utilized in the fabrication of FGM, and they are rather expensive.

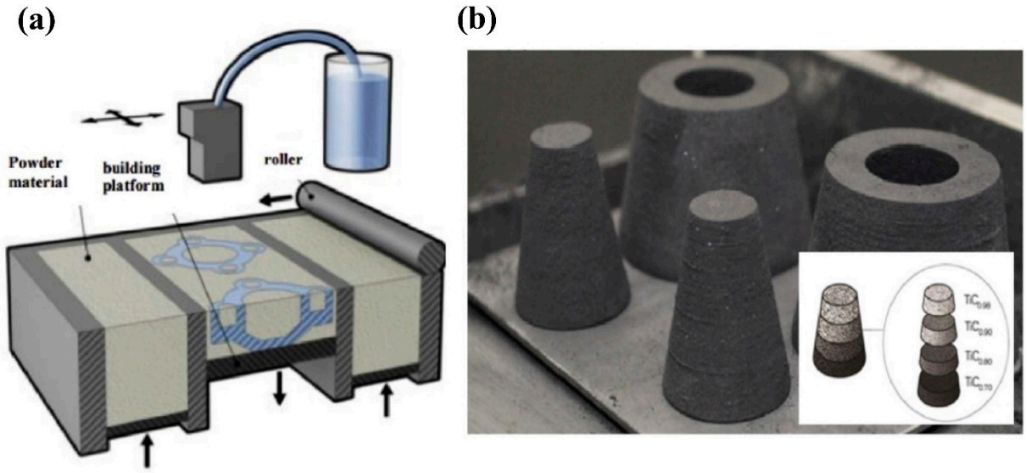

Figure 14. (**a**) Schematic of a material jetting process. "Reprinted with permission from [209]. Copyright 2019 Elsevier."; and (**b**) TiC/steel FGMs processed by material jetting process. "Reprinted with permission from [219]. Copyright 2017 Elsevier".

9. Conclusions and Future Directions

Recent progress in the homogenization methods, representation techniques, modeling, analysis, optimization, and manufacturing of FGM with complex material composition distributions has been reviewed in this paper. Because FGM is such a large and fast evolving field, these findings will not be able to cover all important directions, trends, and needs. Some of the current issues and future developments in FGM structure design are recognized and included by the authors based on the published research and their own analysis of the subject.

1. With the advent of AM, FGM with a complex geometry and material distribution can be fabricated. To get the most out of this, we need advanced methodologies to design and fabricate parts with optimal material distributions and/or geometries.
2. The development of a data-driven strategy to complement designers' creativity and knowledge would be a fascinating area of future work. The first step in establishing a data-driven approach would be to build a massive database of material models and their attributes. The physical and mechanical properties of various combinations of materials in various compositions should be tested and maintained in the database. The database could be used to generate automated suggestions pertaining to the materials to be used for different portions of the designs, the composition of materials to be used, and other topological and geometrical changes to the design using suggestive techniques developed with machine learning and probabilistic models for the CAD domain.
3. To analyze and simulate the behavior of more complicated FGM objects, advanced and resilient numerical approaches as well as a representation scheme that facilitates analytical calculations must be devised. Furthermore, having a system that can optimize and recommend relevant adjustments in the design to satisfy and meet the designers' needs would be quite advantageous. The recommended alterations could take the form of changes to the design's geometrical characteristics, topology, or material distribution over crucial sections.
4. Because the progressive and smooth changing of material constituents is a major aspect of FGMs, the most common design variable in the examined studies was the material distribution pattern. The manufacturability of the FG structure was taken into consideration in a few optimization experiments. It's a good idea to include manufacturability in the optimization studies because it leads to more practical designs with a better chance of being mass produced.
5. So far, several AM technologies have been proposed to manufacture FGMs. Real-world industrial applications, on the other hand, are still few and far between, necessitating major and thorough research efforts to address the vast array of concerns and obstacles involved. As new functional materials with complicated compositions arise, new sophisticated manufacturing technologies, including new procedures for the fabrication of FGMs, must be developed. Micro-nano additive manufacturing (sometimes referred to as micro-nano scale 3D printing) is a new processing technique for producing sophisticated micro-nano structures. High aspect ratio micro-nano structures, multi-lateral micro-nano structures, macro/micro-composite structures, and embedded hetero-structures are all possible using FGAM.

In closing, despite the challenges that remain, it is evident that the field of AM and more specifically as applied to FGMs, offers huge potential. Through precise control of compositions, components, and structures at different length-scales, as well as the integration of numerous gradients, FGM is opening up new pathways for manufacturing innovative functional materials with intricate gradients and highly specialized characteristics. Such advanced multi-materials are predicted to be utilized in the construction of innovative three-dimensional structures and FG devices in the not-too-distant future. However, it is evident that there is still a significant amount of research to be done.

Author Contributions: Investigation, P.N. and A.A.; writing—original draft preparation, P.N.; writing—review and editing, A.A. All authors have read and agreed to the published version of the manuscript.

Funding: This research received no external funding.

Institutional Review Board Statement: Not applicable.

Data Availability Statement: Not applicable.

Conflicts of Interest: The authors declare no conflict of interest.

Nomenclature

Symbols

E	Young's modulus
E_t	tangent modulus
K	bulk modulus
k	thermal conductivity
P	material properties
q	ratio of stress to strain transfer
s_y	yield strength
T	temperature
V	volume fraction

Greek letters

α	coefficient of thermal expansion
μ	shear modulus
ν	Poisson's ratio
ε	strain
σ	stress

Abbreviations

AEH	asymptotic expansion homogenization
AHEFA	adaptive hybrid evolutionary firefly algorithm
AM	additive manufacturing
ANN	artificial neural network
BFG	bidirectional functionally graded
CAMD	continuous approximation of material distribution
CPU	central processing unit
CSG	constructive solid geometry
CT	computerized tomography
CUF	Carrera's unified formulation
DE	differential evolution
DED	direct energy deposition
DLMD	direct laser metal deposition
DMSh	direct multi-search
DNN	deep neural network
EFG	element-free Galerkin
FA	firefly algorithm
FDM	finite difference method
FEA	finite element analysis
FEM	finite element method
FG	functionally graded
FGM	functionally graded materials
FGS	functionally graded sandwich
FSDT	first-order shear deformation theory
GA	genetic algorithm
HAP	hydroxyapatite
HSDT	higher-order shear deformation theory
IGA	isogeometric analysis
IMD	isogeometric multi-mesh design
LMD	laser metal deposition
MAT	medial axis transform
mSOS	modified symbiotic organisms search
NSGA	non-dominated sorting genetic algorithm
NURBS	non-uniform rational B-splines
PSO	particle swarm optimization
RVE	representative volume element
SA	simulated annealing
SOS	symbiotic organism search
SQP	sequential quadratic programming
TSDT	third-order shear deformation theory
X-FEM	extended finite element method

References

1. Inácio, P.L.; Camacho, E.F.; Schell, N.; Fernandes, F.B.; Oliveira, J.; Santos, T.G. Production and characterization of functionally graded NiTi shape memory alloys by Joule effect. *J. Mater. Process. Technol.* **2020**, *285*, 116803. [CrossRef]
2. Rodrigues, T.A.; Bairrão, N.; Farias, F.W.C.; Shamsolhodaei, A.; Shen, J.; Zhou, N.; Maawad, E.; Schell, N.; Santos, T.G.; Oliveira, J. Steel-copper functionally graded material produced by twin-wire and arc additive manufacturing (T-WAAM). *Mater. Des.* **2021**, *213*, 110270. [CrossRef]
3. Torquato, S. *Random Heterogeneous Materials*; Springer: Berlin/Heidelberg, Germany, 2002. [CrossRef]
4. Swaminathan, K.; Naveenkumar, D.T.; Zenkour, A.M.; Carrera, E. Stress, vibration and buckling analyses of FGM plates—A state-of-the-art review. *Compos. Struct.* **2015**, *120*, 10–31. [CrossRef]

5. Lewis, R.W.; Ravindren, K. Finite element simulation of metal casting. *Int. J. Numer. Methods Eng.* **2000**, *47*, 29–59. [CrossRef]
6. Koizumi, M. FGM activities in Japan. *Compos. Part B Eng.* **1997**, *28*, 1–4. [CrossRef]
7. Erdogan, F. Fracture mechanics of functionally graded materials. *Compos. Eng.* **1995**, *5*, 753–770. [CrossRef]
8. Naebe, M.; Shirvanimoghaddam, K. Functionally graded materials: A review of fabrication and properties. *Appl. Mater. Today* **2016**, *5*, 223–245. [CrossRef]
9. Liew, K.; Lei, Z.; Zhang, L. Mechanical analysis of functionally graded carbon nanotube reinforced composites: A review. *Compos. Struct.* **2015**, *120*, 90–97. [CrossRef]
10. Jha, D.K.; Kant, T.; Singh, R.K. A critical review of recent research on functionally graded plates. *Compos. Struct.* **2013**, *96*, 833–849. [CrossRef]
11. Reddy, J. Microstructure-dependent couple stress theories of functionally graded beams. *J. Mech. Phys. Solids* **2011**, *59*, 2382–2399. [CrossRef]
12. Asghari, M.; Ahmadian, M.; Kahrobaiyan, M.; Rahaeifard, M. On the size-dependent behavior of functionally graded micro-beams. *Mater. Des.* **2010**, *31*, 2324–2329. [CrossRef]
13. Birman, V.; Byrd, L.W. Modeling and Analysis of Functionally Graded Materials and Structures. *Appl. Mech. Rev.* **2007**, *60*, 195–216. [CrossRef]
14. Kieback, B.; Neubrand, A.; Riedel, H. Processing techniques for functionally graded materials. *Mater. Sci. Eng. A* **2003**, *362*, 81–106. [CrossRef]
15. Vaezi, M.; Chianrabutra, S.; Mellor, B.; Yang, S. Multiple material additive manufacturing—Part 1: A review. *Virtual Phys. Prototyp.* **2013**, *8*, 19–50. [CrossRef]
16. Ngo, T.D.; Kashani, A.; Imbalzano, G.; Nguyen, K.T.Q.; Hui, D. Additive Manufacturing (3D Printing): A Review of Materials, Methods, Applications and Challenges. *Compos. Part B Eng.* **2018**, *143*, 172–196. [CrossRef]
17. Li, Y.; Feng, Z.; Hao, L.; Huang, L.; Xin, C.; Wang, Y.; Bilotti, E.; Essa, K.; Zhang, H.; Li, Z.; et al. A Review on Functionally Graded Materials and Structures via Additive Manufacturing: From Multi-Scale Design to Versatile Functional Properties. *Adv. Mater. Technol.* **2020**, *5*. [CrossRef]
18. Kou, X.; Tan, S. Heterogeneous object modeling: A review. *Comput. Des.* **2007**, *39*, 284–301. [CrossRef]
19. Mortensen, A.; Suresh, S. Functionally graded metals and metal-ceramic composites: Part 1 Processing. *Int. Mater. Rev.* **1995**, *40*, 239–265. [CrossRef]
20. Suresh, S.; Mortensen, A. Functionally graded metals and metal-ceramic composites: Part 2 Thermomechanical behaviour. *Int. Mater. Rev.* **1997**, *42*, 85–116. [CrossRef]
21. Bever, M.B.; Duwez, P.E. Gradients in composite materials. *Mater. Sci. Eng.* **1972**, *10*, 1–8. [CrossRef]
22. Shen, M.; Bever, M.B. Gradients in polymeric materials. *J. Mater. Sci.* **1972**, *7*, 741–746. [CrossRef]
23. Koizumi, M. The Concept of FGM, in second International Symposium on functionally gradient materials (ed. Holt, J.B., Koizumi, M., Hirai, T. and Munir, Z.A.). *J. Am. Ceram. Soc.* **1992**, 3–10.
24. Koizumi, M.; Niino, M. Overview of FGM Research in Japan. *MRS Bull.* **1995**, *20*, 19–21. [CrossRef]
25. Uemura, S. The Activities of FGM on New Application. *Mater. Sci. Forum* **2003**, *423–425*, 1–10. [CrossRef]
26. Saleh, B.; Jiang, J.; Fathi, R.; Al-Hababi, T.; Xu, Q.; Wang, L.; Song, D.; Ma, A. 30 Years of functionally graded materials: An overview of manufacturing methods, Applications and Future Challenges. *Compos. Part B Eng.* **2020**, *201*, 108376. [CrossRef]
27. Noda, N.; Tsuji, T. Steady thermal stresses in a plate of functionally gradient material. *Trans. Jpn. Soc. Mech. Eng. Ser. A* **1991**, *57*, 98–103. [CrossRef]
28. Arai, Y.; Kobayashi, H.; Tamura, M. Elastic-Plastic Thermal Stress Analysis for Optimum Material Design of Functionally Gradient Material. *Trans. Jpn. Soc. Mech. Eng. Ser. A* **1993**, *59*, 849–855. [CrossRef]
29. Erdogan, F.; Kaya, A.C.; Joseph, P.F. The Crack Problem in Bonded Nonhomogeneous Materials. *J. Appl. Mech.* **1991**, *58*, 410–418. [CrossRef]
30. Noda, N.; Jin, Z.-H. A crack in functionally gradient materials under thermal shock. *Ing.-Arch.* **1994**, *64*, 99–110. [CrossRef]
31. Clements, D.L.; Kusuma, J.; Ang, W.-T. A note on antiplane deformations of inhomogeneous elastic materials. *Int. J. Eng. Sci.* **1997**, *35*, 593–601. [CrossRef]
32. Nemat-Alla, M.; Noda, N. Thermal stress intensity factor for functionally gradient half space with an edge crack under thermal load. *Arch. Appl. Mech.* **1996**, *66*, 569–580. [CrossRef]
33. Nemat-Alla, M.; Noda, N. Study of an Edge Crack Problem in a Semi-Infinite functionally graded medium with Two Deviensionally Nonhomogeneous Coefficients of Thermal Expansion under Thermal Load. *J. Therm. Stress.* **1996**, *19*, 863–888. [CrossRef]
34. Nemat-Alla, M.; Noda, N. Edge crack problem in a semi-infinite FGM plate with a bi-directional coefficient of thermal expansion under two-dimensional thermal loading. *Acta Mech.* **2000**, *144*, 211–229. [CrossRef]
35. Marin, L. Numerical solution of the Cauchy problem for steady-state heat transfer in two-dimensional functionally graded materials. *Int. J. Solids Struct.* **2005**, *42*, 4338–4351. [CrossRef]
36. Ke, L.-L.; Wang, Y.-S. Two-dimensional contact mechanics of functionally graded materials with arbitrary spatial variations of material properties. *Int. J. Solids Struct.* **2006**, *43*, 5779–5798. [CrossRef]
37. Aboudi, J.; Pindera, M.-J.; Arnold, S. Higher-order theory for functionally graded materials. *Compos. Part B Eng.* **1999**, *30*, 777–832. [CrossRef]

38. Aboudi, J.; Pindera, M.-J.; Arnold, S.M. Thermoelastic theory for the response of materials functionally graded in two directions. *Int. J. Solids Struct.* **1996**, *33*, 931–966. [CrossRef]
39. Aboudi, J.; Pindera, M.-J.; Arnold, S.M. Thermo Plasticity Theory for Bidirectionally Functionally Graded Materials. *J. Therm. Stress.* **1996**, *19*, 809–861. [CrossRef]
40. Cho, J.; Ha, D. Optimal tailoring of 2D volume-fraction distributions for heat-resisting functionally graded materials using FDM. *Comput. Methods Appl. Mech. Eng.* **2002**, *191*, 3195–3211. [CrossRef]
41. Goupee, A.J.; Vel, S.S. Two-dimensional optimization of material composition of functionally graded materials using meshless analyses and a genetic algorithm. *Comput. Methods Appl. Mech. Eng.* **2006**, *195*, 5926–5948. [CrossRef]
42. Nemat-Alla, M. Reduction of thermal stresses by developing two-dimensional functionally graded materials. *Int. J. Solids Struct.* **2003**, *40*, 7339–7356. [CrossRef]
43. Nemat-Alla, M.; Ahmed, K.I.; Hassab-Allah, I. Elastic–plastic analysis of two-dimensional functionally graded materials under thermal loading. *Int. J. Solids Struct.* **2009**, *46*, 2774–2786. [CrossRef]
44. Noda, N.; Tsuji, T. Steady thermal stresses in a plate of functionally gradient material with temperature-dependent properties. *Trans. Jpn. Soc. Mech. Eng. Ser. A* **1991**, *57*, 625–631. [CrossRef]
45. Obata, Y.; Noda, N.; Tsuji, T. Steady Thermal Stresses in a Functionally Gradient Material Plate. Influence of Mechanical Boundary Conditions. *Trans. Jpn. Soc. Mech. Eng. Ser. A* **1992**, *58*, 1689–1695. [CrossRef]
46. Obata, Y.; Noda, N. Steady Thermal Stresses in a Hollow Circular Cylinder and a Hollow Sphere of a Functionally Gradient Material. *J. Therm. Stress.* **1994**, *17*, 471–487. [CrossRef]
47. Tanigawa, Y.; Matsumoto, M.; Akai, T. Optimization of Material Composition to Minimize Thermal Stresses in Nonhomogeneous Plate Subjected to Unsteady Heat Supply. *JSME Int. J. Ser. A Mech. Mater. Eng.* **1997**, *40*, 84–93. [CrossRef]
48. Tanigawa, Y.; Oka, N.; Akai, T.; Kawamura, R. One-Dimensional Transient Thermal Stress Problem for Nonhomogeneous Hollow Circular Cylinder and Its Optimization of Material Composition for Thermal Stress Relaxation. *JSME Int. J. Ser. A Mech. Mater. Eng.* **1997**, *40*, 117–127. [CrossRef]
49. Berke, L.; Patnaik, S.; Murthy, P. Optimum design of aerospace structural components using neural networks. *Comput. Struct.* **1993**, *48*, 1001–1010. [CrossRef]
50. Kang, H.-T.; Yoon, C.J. Neural Network Approaches to Aid Simple Truss Design Problems. *Comput. Civ. Infrastruct. Eng.* **1994**, *9*, 211–218. [CrossRef]
51. Hung, S.; Adeli, H. Object-oriented backpropagation and its application to structural design. *Neurocomputing* **1994**, *6*, 45–55. [CrossRef]
52. Yoshimura, S.; Matsuda, A.; Yagawa, G. New regularization by transformation for neural network based inverse analyses and its application to structure identification. *Int. J. Numer. Methods Eng.* **1996**, *39*, 3953–3968. [CrossRef]
53. Tanaka, M.; Hanahara, K.; Seguchi, Y. Configuration Control of the Truss-Type Parallel Manipulator by the Modular Neural Network Model. *JSME Int. J. Ser 3. Vib Control Eng. Eng. Ind.* **1992**, *35*, 89–95. [CrossRef]
54. Ootao, Y.; Kawamura, R.; Tanigawa, Y.; Nakamura, T. Neural network optimization of material composition of a functionally graded material plate at arbitrary temperature range and temperature rise. *Ingenieur-Archiv* **1998**, *68*, 662–676. [CrossRef]
55. Ootao, R.K.Y. Optimization of Material Composition of Nonhomogeneous Hollow Circular Cylinder for Thermal Stress Relaxation Making Use of Neural Network. *J. Therm. Stress.* **1999**, *22*, 1–22. [CrossRef]
56. Ootao, Y.; Kawamura, R.; Tanigawa, Y.; Imamura, R. Optimization of material composition of nonhomogeneous hollow sphere for thermal stress relaxation making use of neural network. *Comput. Methods Appl. Mech. Eng.* **1999**, *180*, 185–201. [CrossRef]
57. Ootao, Y.T.Y. Optimization of Material Composition of Functionally Graded Plate for Thermal Stress Relaxation Using a Genetic Algorithm. *J. Therm. Stress.* **2000**, *23*, 257–271. [CrossRef]
58. Tanaka, K.; Tanaka, Y.; Enomoto, K.; Poterasu, V.; Sugano, Y. Design of thermoelastic materials using direct sensitivity and optimization methods. Reduction of thermal stresses in functionally gradient materials. *Comput. Methods Appl. Mech. Eng.* **1993**, *106*, 271–284. [CrossRef]
59. Tanaka, K.; Watanabe, H.; Sugano, Y.; Poterasu, V. A multicriterial material tailoring of a hollow cylinder in functionally gradient materials: Scheme to global reduction of thermoelastic stresses. *Comput. Methods Appl. Mech. Eng.* **1996**, *135*, 369–380. [CrossRef]
60. Lipton, R. Design of functionally graded composite structures in the presence of stress constraints. *Int. J. Solids Struct.* **2002**, *39*, 2575–2586. [CrossRef]
61. Turteltaub, S. Optimal control and optimization of functionally graded materials for thermomechanical processes. *Int. J. Solids Struct.* **2002**, *39*, 3175–3197. [CrossRef]
62. Turteltaub, S. Functionally graded materials for prescribed field evolution. *Comput. Methods Appl. Mech. Eng.* **2002**, *191*, 2283–2296. [CrossRef]
63. Cho, J.; Choi, J. A yield-criteria tailoring of the volume fraction in metal-ceramic functionally graded material. *Eur. J. Mech.-A/Solids* **2004**, *23*, 271–281. [CrossRef]
64. Arslan, K.; Gunes, R.; Apalak, M.K.; Reddy, J.N. Evaluation of geometrically nonlinear and elastoplastic behavior of functionally graded plates under mechanical loading–unloading. *Mech. Adv. Mater. Struct.* **2020**, *29*, 1587–1600. [CrossRef]
65. Huang, J.; Fadel, G.M.; Blouin, V.Y.; Grujicic, M. Bi-objective optimization design of functionally gradient materials. *Mater. Des.* **2002**, *23*, 657–666. [CrossRef]

66. Goupee, A.J.; Vel, S.S. Multi-objective optimization of functionally graded materials with temperature-dependent material properties. *Mater. Des.* **2007**, *28*, 1861–1879. [CrossRef]
67. Rüter, M.O. *Error Estimates for Advanced Galerkin Methods*; Springer: Berlin/Heidelberg, Germany, 2019; pp. 75–148. [CrossRef]
68. Vel, S.; Goupee, A.J. Multi-objective Optimization of Geometric Dimensions and Material Composition of Functionally Graded Components. In *AIP Conference Proceedings*; AIP Publishing LLC: Melville, NY, USA, 2008. [CrossRef]
69. Lin, D.; Li, Q.; Li, W.; Zhou, S.; Swain, M.V. Design optimization of functionally graded dental implant for bone remodeling. *Compos. Part B Eng.* **2009**, *40*, 668–675. [CrossRef]
70. Cheng, Z.-Q.; Batra, R. Three-dimensional thermoelastic deformations of a functionally graded elliptic plate. *Compos. Part B Eng.* **2000**, *31*, 97–106. [CrossRef]
71. Mori, T.; Tanaka, K. Average stress in matrix and average elastic energy of materials with misfitting inclusions. *Acta Met.* **1973**, *21*, 571–574. [CrossRef]
72. Praveen, G.N.; Reddy, J.N. Nonlinear transient thermoelastic analysis of functionally graded ramic–metal plates. *Int. J. Solids Struct.* **1998**, *35*, 4457–4476. [CrossRef]
73. Reddy, J.; Cheng, Z.-Q. Three-dimensional thermomechanical deformations of functionally graded rectangular plates. *Eur. J. Mech.-A/Solids* **2001**, *20*, 841–855. [CrossRef]
74. Carrera, E.; Brischetto, S.; Robaldo, A. Variable Kinematic Model for the Analysis of Functionally Graded Material plates. *AIAA J.* **2008**, *46*, 194–203. [CrossRef]
75. Carrera, E. Theories and Finite Elements for Multilayered Plates and Shells:A Unified compact formulation with numerical assessment and benchmarking. *Arch. Comput. Methods Eng.* **2003**, *10*, 215–296. [CrossRef]
76. Almeida, S.R.M.; Paulino, G.H.; Silva, E.C.N. Layout and material gradation in topology optimization of functionally graded structures: A global–local approach. *Struct. Multidiscip. Optim.* **2010**, *42*, 855–868. [CrossRef]
77. Noh, Y.; Kang, Y.; Youn, S.; Cho, J.; Lim, O. Reliability-based design optimization of volume fraction distribution in functionally graded composites. *Comput. Mater. Sci.* **2013**, *69*, 435–442. [CrossRef]
78. Nabian, M.; Ahmadian, M.T. Multi-Objective Optimization of Functionally Graded Hollow Cylinders. In Proceedings of the ASME 2011 International Mechanical Engineering Congress and Exposition, Denver, Colorado, USA, 11–17 November 2011; pp. 583–590. [CrossRef]
79. Nouri, A.; Astaraki, S. Optimization of Sound Transmission Loss through a Thin Functionally Graded Material Cylindrical Shell. *Shock Vib.* **2014**, *2014*, 1–10. [CrossRef]
80. Xu, Y.; Zhang, W.; Chamoret, D.; Domaszewski, M. Minimizing thermal residual stresses in C/SiC functionally graded material coating of C/C composites by using particle swarm optimization algorithm. *Comput. Mater. Sci.* **2012**, *61*, 99–105. [CrossRef]
81. Kou, X.; Tan, S. Microstructural modelling of functionally graded materials using stochastic Voronoi diagram and B-Spline representations. *Int. J. Comput. Integr. Manuf.* **2012**, *25*, 177–188. [CrossRef]
82. Chiba, R.; Sugano, Y. Optimisation of material composition of functionally graded materials based on multiscale thermoelastic analysis. *Acta Mech.* **2012**, *223*, 891–909. [CrossRef]
83. Ghazanfari, A.; Leu, M.C. Composition Optimization for Functionally Gradient Parts Considering Manufacturing Constraints. In Proceedings of the ASME 2014 International Manufacturing Science and Engineering Conference collocated with the JSME 2014 International Conference on Materials and Processing and the 42nd North American Manufacturing Research Conference, Detroit, MI, USA, 9–13 June 2014. [CrossRef]
84. Reddy, J.N.; Chin, C.D. Thermomechanical analysis of functionally graded cylinders and plates. *J. Therm. Stress.* **1998**, *21*, 593–626. [CrossRef]
85. Bahraminasab, M.; Bin Sahari, B.; Edwards, K.; Farahmand, F.; Hong, T.S.; Arumugam, M.; Jahan, A. Multi-objective design optimization of functionally graded material for the femoral component of a total knee replacement. *Mater. Des.* **2013**, *53*, 159–173. [CrossRef]
86. Lieu, Q.X.; Lee, J. Modeling and optimization of functionally graded plates under thermo-mechanical load using isogeometric analysis and adaptive hybrid evolutionary firefly algorithm. *Compos. Struct.* **2017**, *179*, 89–106. [CrossRef]
87. Correia, V.M.F.; Madeira, J.A.; Araújo, A.L.; Soares, C.M.M. Multiobjective optimization of functionally graded material plates with thermo-mechanical loading. *Compos. Struct.* **2018**, *207*, 845–857. [CrossRef]
88. Moleiro, F.; Madeira, J.; Carrera, E.; Reddy, J. Design optimization of functionally graded plates under thermo-mechanical loadings to minimize stress, deformation and mass. *Compos. Struct.* **2020**, *245*, 112360. [CrossRef]
89. Qu, Y.; Jin, F.; Zhang, G. Mechanically induced electric and magnetic fields in the bending and symmetric-shear deformations of a microstructure-dependent FG-MEE composite beam. *Compos. Struct.* **2021**, *278*, 114554. [CrossRef]
90. Boccaccio, A.; Uva, A.; Fiorentino, M.; Mori, G.; Monno, G. Geometry Design Optimization of Functionally Graded Scaffolds for Bone Tissue Engineering: A Mechanobiological Approach. *PLoS ONE* **2016**, *11*, e0146935. [CrossRef]
91. Boccaccio, A.; Uva, A.; Fiorentino, M.; Lamberti, L.; Monno, G. A Mechanobiology-based Algorithm to Optimize the Microstructure Geometry of Bone Tissue Scaffolds. *Int. J. Biol. Sci.* **2016**, *12*, 1–17. [CrossRef]
92. Das, S.; Sutradhar, A. Multi-physics topology optimization of functionally graded controllable porous structures: Application to heat dissipating problems. *Mater. Des.* **2020**, *193*, 108775. [CrossRef]
93. Wang, Y.; Arabnejad, S.; Tanzer, M.; Pasini, D. Hip Implant Design With Three-Dimensional Porous Architecture of Optimized Graded Density. *J. Mech. Des.* **2018**, *140*. [CrossRef]

94. Aage, N.; Andreassen, E.; Lazarov, B.S.; Sigmund, O. Giga-voxel computational morphogenesis for structural design. *Nature* **2017**, *550*, 84–86. [CrossRef]
95. Lee, Y.-S.; González, J.A.; Lee, J.H.; Kim, Y.I.; Park, K.; Han, S. Structural topology optimization of the transition piece for an offshore wind turbine with jacket foundation. *Renew. Energy* **2016**, *85*, 1214–1225. [CrossRef]
96. Magerramova, L.; Vasilyev, B.; Kinzburskiy, V. Novel Designs of Turbine Blades for Additive Manufacturing. In Proceedings of the Volume 5C: Heat Transfer; ASME International: New York, NY, USA, 2016; pp. 1–7.
97. Zhang, F.; Zhou, C.; Das, S. An Efficient Design Optimization Method for Functional Gradient Material Objects Based on Finite Element Analysis. In Proceedings of the International Design Engineering Technical Conferences and Computers and Information in Engineering Conference, Boston, MA, USA, 2–5 August 2015. [CrossRef]
98. Gupta, A.; Talha, M. Recent development in modeling and analysis of functionally graded materials and structures. *Prog. Aerosp. Sci.* **2015**, *79*, 1–14. [CrossRef]
99. Gibson, L.J.; Ashby, M.F.; Karam, G.N.; Wegst, U.G.; Shercliff, H.R. The mechanical properties of natural materials. II. Microstructures for mechanical efficiency. *Proc. R. Soc. Lond. A* **1995**, *450*, 141–162. [CrossRef]
100. Van Do, T.; Nguyen, D.K.; Duc, N.D.; Doan, D.H.; Bui, T.Q. Analysis of bi-directional functionally graded plates by FEM and a new third-order shear deformation plate theory. *Thin-Walled Struct.* **2017**, *119*, 687–699. [CrossRef]
101. Zghal, S.; Frikha, A.; Dammak, F. Mechanical buckling analysis of functionally graded power-based and carbon nanotubes-reinforced composite plates and curved panels. *Compos. Part B Eng.* **2018**, *150*, 165–183. [CrossRef]
102. Cho, J.R.; Ha, D.Y. Volume fraction optimization for minimizing thermal stress in Ni–Al2O3 functionally graded materials. *Mater. Sci. Eng. A* **2002**, *334*, 147–155. [CrossRef]
103. Hirshikesh; Natarajan, S.; Annabattula, R.K.; Martínez-Pañeda, E. Phase field modelling of crack propagation in functionally graded materials. *Compos. Part B Eng.* **2019**, *169*, 239–248. [CrossRef]
104. Srividhya, S.; Basant, K.; Gupta, R.K.; Rajagopal, A.; Reddy, J.N. Influence of the homogenization scheme on the bending response of functionally graded plates. *Acta Mech.* **2018**, *229*, 4071–4089. [CrossRef]
105. Hashin, Z.; Shtrikman, S. A Variational Approach to the Theory of the Effective Magnetic Permeability of Multiphase Materials. *J. Appl. Phys.* **1962**, *33*, 3125–3131. [CrossRef]
106. Norris, A.N. An Examination of the Mori-Tanaka Effective Medium Approximation for Multiphase Composites. *J. Appl. Mech.* **1989**, *56*, 83–88. [CrossRef]
107. Liu, C.; Qian, R.; Liu, Z.; Liu, G.; Zhang, Y. Multi-scale modelling of thermal conductivity of phase change material/recycled cement paste incorporated cement-based composite material. *Mater. Des.* **2020**, *191*, 108646. [CrossRef]
108. Levin, V.M. On the coefficients of thermal expansion of heterogeneous materials. *Mech. Solids.* **1967**, *2*, 58–61.
109. Lages, E.N.; Marques, S.P.C. Thermoelastic homogenization of periodic composites using an eigenstrain-based micromechanical model. *Appl. Math. Model.* **2020**, *85*, 1–18. [CrossRef]
110. Eshelby, J.D. The determination of the elastic field of an ellipsoidal inclusion, and related problems. *Proc. R. Soc. Lond. Ser. A Math. Phys. Sci.* **1957**, *241*, 376–396. [CrossRef]
111. Jackson, G.R.; Smith, K.; McCarthy, P.C.; Fisher, T. Modeling Thermal Storage in Wax-Impregnated Foams with a Pore-Scale Submodel. *J. Thermophys. Heat Transf.* **2015**, *29*, 812–819. [CrossRef]
112. Pietrak, K.; Wiśniewski, T. A review of models for effective thermal conductivity of composite materials. *J. Power Technol.* **2015**, *95*, 14–24.
113. Hasselman, D.; Johnson, L.F. Effective Thermal Conductivity of Composites with Interfacial Thermal Barrier Resistance. *J. Compos. Mater.* **1987**, *21*, 508–515. [CrossRef]
114. Maxwell, J.C. *A Treatise on Electricity and Magnetism*; Clarendon Press: Oxford, UK; London, UK, 1873.
115. Sevostianov, I.; Bruno, G. Maxwell scheme for internal stresses in multiphase composites. *Mech. Mater.* **2018**, *129*, 320–331. [CrossRef]
116. Snarskii, A.A.; Shamonin, M.; Yuskevich, P. Effective Medium Theory for the Elastic Properties of Composite Materials with Various Percolation Thresholds. *Materials* **2020**, *13*, 1243. [CrossRef]
117. Kanaun, S.; Levin, V. *Effective Field Method in the Theory of Heterogeneous Media*; Springer: Berlin/Heidelberg, Germany, 2013; Volume 193, pp. 199–282. [CrossRef]
118. Rodríguez-Ramos, R.; Gandarilla-Pérez, C.A.; Lau-Alfonso, L.; Lebon, F.; Sabina, F.J.; Sevostianov, I. Maxwell homogenization scheme for piezoelectric composites with arbitrarily-oriented spheroidal inhomogeneities. *Acta Mech.* **2019**, *230*, 3613–3632. [CrossRef]
119. Berryman, J.G.; Berge, P.A. Critique of two explicit schemes for estimating elastic properties of multiphase composites. *Mech. Mater.* **1996**, *22*, 149–164. [CrossRef]
120. Touloukian, Y.S. *Thermophysical Properties of High Temperature Solid Materials*; Macmillan Company: New York, NY, USA, 1967.
121. Sun, C.; Vaidya, R. Prediction of composite properties from a representative volume element. *Compos. Sci. Technol.* **1996**, *56*, 171–179. [CrossRef]
122. Chao, X.; Qi, L.; Cheng, J.; Tian, W.; Zhang, S.; Li, H. Numerical evaluation of the effect of pores on effective elastic properties of carbon/carbon composites. *Compos. Struct.* **2018**, *196*, 108–116. [CrossRef]
123. Qi, L.; Chao, X.; Tian, W.; Ma, W.; Li, H. Numerical study of the effects of irregular pores on transverse mechanical properties of unidirectional composites. *Compos. Sci. Technol.* **2018**, *159*, 142–151. [CrossRef]

124. Mohan, P.K.; Kumar, M.A.; Mohite, P. Representative volume element generation and its size determination for discontinuous composites made from chopped prepregs. *Compos. Struct.* **2020**, *252*, 112633. [CrossRef]
125. Raju, B.; Hiremath, S.; Mahapatra, D.R. A review of micromechanics based models for effective elastic properties of reinforced polymer matrix composites. *Compos. Struct.* **2018**, *204*, 607–619. [CrossRef]
126. Naik, R.; Crews, J. *Micromechanical Analysis of Fiber-Matrix Interface Stresses Under Thermomechanical Loadings*; ASTM Special Technical Publication: West Conshohocken, PA, USA, 1993; Volume 1206, p. 205. [CrossRef]
127. Tamura, I.; Tomota, Y.; Ozawa, M. Strength and ductility of Fe–Ni–C alloys composed of austenite and martensite with various strength. In Proceedings of the Third Int Conf Strength Met Alloy, Cambridge, MA, USA, 20–25 August 1973; pp. 611–615.
128. Nakamura, T.; Wang, T.; Sampath, S. Determination of properties of graded materials by inverse analysis and instrumented indentation. *Acta Mater.* **2000**, *48*, 4293–4306. [CrossRef]
129. Jin, Z.-H.; Paulino, G.H.; Dodds, R.H. Cohesive fracture modeling of elastic–plastic crack growth in functionally graded materials. *Eng. Fract. Mech.* **2003**, *70*, 1885–1912. [CrossRef]
130. Huang, H.; Chen, B.; Han, Q. Investigation on buckling behaviors of elastoplastic functionally graded cylindrical shells subjected to torsional loads. *Compos. Struct.* **2014**, *118*, 234–240. [CrossRef]
131. Nayak, P.; Bhowmick, S.; Saha, K.N. Elasto-plastic analysis of thermo-mechanically loaded functionally graded disks by an iterative variational method. *Eng. Sci. Technol. Int. J.* **2019**, *23*, 42–64. [CrossRef]
132. Nikbakht, S.; Salami, S.J.; Shakeri, M. Three dimensional analysis of functionally graded plates up to yielding, using full layer-wise finite element method. *Compos. Struct.* **2017**, *182*, 99–115. [CrossRef]
133. Komarsofla, M.K.; Salami, S.J.; Shakeri, M. Thermo elastic-up to yielding behavior of three dimensional functionally graded cylindrical panel based on a full layer-wise theory. *Compos. Struct.* **2018**, *208*, 261–275. [CrossRef]
134. Zhang, B.; Jaiswal, P.; Rai, R.; Nelaturi, S. Additive Manufacturing of Functionally Graded Material Objects: A Review. *J. Comput. Inf. Sci. Eng.* **2018**, *18*. [CrossRef]
135. Li, B.; Fu, J.; Feng, J.; Shang, C.; Lin, Z. Review of heterogeneous material objects modeling in additive manufacturing. *Vis. Comput. Ind. Biomed. Art* **2020**, *3*, 1–18. [CrossRef] [PubMed]
136. Ueng, S.-K.; Chen, L.-G.; Jen, S.-Y. Voxel-based virtual manufacturing simulation for three-dimensional printing. *Adv. Mech. Eng.* **2018**, *10*. [CrossRef]
137. Aremu, A.; Brennan-Craddock, J.; Panesar, A.S.; Ashcroft, I.; Hague, R.; Wildman, R.; Tuck, C. A voxel-based method of constructing and skinning conformal and functionally graded lattice structures suitable for additive manufacturing. *Addit. Manuf.* **2016**, *13*, 1–13. [CrossRef]
138. Sossou, G.; Demoly, F.; Belkebir, H.; Qi, H.J.; Gomes, S.; Montavon, G. Design for 4D printing: A voxel-based modeling and simulation of smart materials. *Mater. Des.* **2019**, *175*, 107798. [CrossRef]
139. Jackson, T.R. Analysis of Functionally Graded Material Object Representation Methods. Ph.D. Thesis, Massachusetts Institute of Technology, Cambridge, MA, USA, 2000. Available online: http://hdl.handle.net/1721.1/9032 (accessed on 3 August 2022).
140. You, Y.; Kou, X.; Tan, S. Adaptive meshing for finite element analysis of heterogeneous materials. *Comput. Des.* **2015**, *62*, 176–189. [CrossRef]
141. Saini, A.; Unnikrishnakurup, S.; Krishnamurthy, C.; Balasubramanian, K.; Sundararajan, T. Numerical study using finite element method for heat conduction on heterogeneous materials with varying volume fraction, shape and size of fillers. *Int. J. Therm. Sci.* **2020**, *159*, 106545. [CrossRef]
142. Sharma, G.; Gurumoorthy, B. Modelling multiply connected heterogeneous objects using mixed-dimensional material reference features. *J. Comput. Des. Eng.* **2018**, *6*, 337–347. [CrossRef]
143. Zhu, F.; Chen, K.-Z.; Feng, X.-A. Visualized CAD models of objects made of a multiphase perfect material. *Adv. Eng. Softw.* **2006**, *37*, 20–31. [CrossRef]
144. Nayak, P.; Armani, A. Optimal three-dimensional design of functionally graded parts for additive manufacturing using Tamura–Tomota–Ozawa model. *Proc. Inst. Mech. Eng. Part L: J. Mater. Des. Appl.* **2021**, *235*, 1993–2006. [CrossRef]
145. Ashjari, M.; Khoshravan, M.R. Multi-objective optimization of a functionally graded sandwich panel under mechanical loading in the presence of stress constraint. *J. Mech. Behav. Mater.* **2017**, *26*, 79–93. [CrossRef]
146. Kou, X.; Tan, S. Modeling Functionally Graded Porous Structures with Stochastic Voronoi Diagram and B-Spline Representations. In Proceedings of the 2010 International Conference on Manufacturing Automation, Hong Kong, China, 13–15 December 2010; pp. 99–106. [CrossRef]
147. Hughes, T.; Cottrell, J.; Bazilevs, Y. Isogeometric analysis: CAD, finite elements, NURBS, exact geometry and mesh refinement. *Comput. Methods Appl. Mech. Eng.* **2005**, *194*, 4135–4195. [CrossRef]
148. Do, D.T.; Nguyen-Xuan, H.; Lee, J. Material optimization of tri-directional functionally graded plates by using deep neural network and isogeometric multimesh design approach. *Appl. Math. Model.* **2020**, *87*, 501–533. [CrossRef]
149. Yavari, A.; Abolbashari, M.H. Generalized Thermoelastic Waves Propagation in Non-uniform Rational B-spline Rods Under Quadratic Thermal Shock Loading Using Isogeometric Approach. *Iran. J. Sci. Technol. Trans. Mech. Eng.* **2020**, *46*, 43–59. [CrossRef]
150. Phung-Van, P.; Ferreira, A.; Thai, C.H. Computational optimization for porosity-dependent isogeometric analysis of functionally graded sandwich nanoplates. *Compos. Struct.* **2020**, *239*, 112029. [CrossRef]
151. Pasko, A.; Adzhiev, V.; Schmitt, B.; Schlick, C. Constructive Hypervolume Modeling. *Graph. Model.* **2001**, *63*, 413–442. [CrossRef]

152. Wang, M.Y.; Wang, X. A level-set based variational method for design and optimization of heterogeneous objects. *Comput. Des.* **2005**, *37*, 321–337. [CrossRef]
153. Singh, S.K.; Tandon, P. Heterogeneous modeling based prosthesis design with porosity and material variation. *J. Mech. Behav. Biomed. Mater.* **2018**, *87*, 124–131. [CrossRef]
154. Ameta, G.; Witherell, P. Representation of Graded Materials and Structures to Support Tolerance Specification for Additive Manufacturing Application. *J. Comput. Inf. Sci. Eng.* **2019**, *19*. [CrossRef]
155. Gupta, V.; Tandon, P. Heterogeneous object modeling with material convolution surfaces. *Comput. Des.* **2015**, *62*, 236–247. [CrossRef]
156. Sharma, G.K.; Gurumoorthy, B. Iso-material contour representation for process planning of heterogeneous object model. *J. Comput. Des. Eng.* **2020**, *7*, 498–513. [CrossRef]
157. Martínez-Pañeda, E.; Gallego, R. Numerical analysis of quasi-static fracture in functionally graded materials. *Int. J. Mech. Mater. Des.* **2014**, *11*, 405–424. [CrossRef]
158. Ramírez-Gil, F.J.; Murillo-Cardoso, J.E.; Silva, E.C.N.; Montealegre-Rubio, W. Optimization of Functionally Graded Materials Considering Dynamical Analysis. *Adv. Struct. Mater.* **2016**, *49*, 205–237. [CrossRef]
159. Ghazanfari, A. Optimal Design and Freeform Extrusion Fabrication of Functionally Gradient Smart Parts. *Ph.D. Thesis*; Missouri University of Science and Technology: Rolla, MO, USA, 2017. Available online: https://scholarsmine.mst.edu/doctoral_dissertations/2594 (accessed on 3 August 2022).
160. Zhou, W.; Ai, S.; Chen, M.; Zhang, R.; He, R.; Pei, Y.; Fang, D. Preparation and thermodynamic analysis of the porous ZrO2/(ZrO2 + Ni) functionally graded bolted joint. *Compos. Part B Eng.* **2015**, *82*, 13–22. [CrossRef]
161. Zhou, W.; Zhang, R.; Ai, S.; He, R.; Pei, Y.; Fang, D. Load distribution in threads of porous metal–ceramic functionally graded composite joints subjected to thermomechanical loading. *Compos. Struct.* **2015**, *134*, 680–688. [CrossRef]
162. Medeiros, M.S.; Parente, E. MicroFEA 1.0—A software package for Finite Element Analysis of functionally graded materials. *SoftwareX* **2020**, *11*, 100481. [CrossRef]
163. Li, D.; Liao, W.; Dai, N.; Dong, G.; Tang, Y.; Xie, Y.M. Optimal design and modeling of gyroid-based functionally graded cellular structures for additive manufacturing. *Comput. Des.* **2018**, *104*, 87–99. [CrossRef]
164. Cheng, L.; Bai, J.; To, A.C. Functionally graded lattice structure topology optimization for the design of additive manufactured components with stress constraints. *Comput. Methods Appl. Mech. Eng.* **2018**, *344*, 334–359. [CrossRef]
165. Burton, H.E.; Eisenstein, N.M.; Lawless, B.M.; Jamshidi, P.; Segarra, M.A.; Addison, O.; Shepherd, D.E.; Attallah, M.; Grover, L.M.; Cox, S.C. The design of additively manufactured lattices to increase the functionality of medical implants. *Mater. Sci. Eng. C* **2018**, *94*, 901–908. [CrossRef]
166. Kladovasilakis, N.; Tsongas, K.; Tzetzis, D. Finite Element Analysis of Orthopedic Hip Implant with Functionally Graded Bioinspired Lattice Structures. *Biomimetics* **2020**, *5*, 44. [CrossRef]
167. Kolahi, M.R.S.; Rahmani, H.; Moeinkhah, H. Mechanical analysis of shrink-fitted thick FG cylinders based on first order shear deformation theory and FE simulation. *Proc. Inst. Mech. Eng. Part C J. Mech. Eng. Sci.* **2021**, *235*, 6388–6397. [CrossRef]
168. Sharma, P.; Singh, R.; Hussain, M. On modal analysis of axially functionally graded material beam under hygrothermal effect. *Proc. Inst. Mech. Eng. Part C J. Mech. Eng. Sci.* **2019**, *234*, 1085–1101. [CrossRef]
169. Zhou, H.M.; Zhang, X.M.; Wang, Z.Y. Thermal Analysis of 2D FGM Beam Subjected to Thermal Loading Using Meshless Weighted Least-Square Method. *Math. Probl. Eng.* **2019**, *2019*, 1–10. [CrossRef]
170. Nguyen, T.-T.; Lee, J. Optimal design of thin-walled functionally graded beams for buckling problems. *Compos. Struct.* **2017**, *179*, 459–467. [CrossRef]
171. Hussien, O.; Mulani, S.B. Two-Dimensional Optimization of Functionally Graded Material Plates Subjected to Buckling Constraints. In Proceedings of the 58th AIAA/ASCE/AHS/ASC Structures, Structural Dynamics, and Materials Conference, Grapevine, TX, USA, 9–13 January 2017. [CrossRef]
172. Correia, V.M.F.; Madeira, J.F.A.; Araújo, A.L.; Soares, C.M.M. Multiobjective optimization of ceramic-metal functionally graded plates using a higher order model. *Compos. Struct.* **2018**, *183*, 146–160. [CrossRef]
173. Moita, J.S.; Araújo, A.L.; Correia, V.F.; Soares, C.M.M.; Herskovits, J. Material distribution and sizing optimization of functionally graded plate-shell structures. *Compos. Part B Eng.* **2018**, *142*, 263–272. [CrossRef]
174. Correia, V.F.; Moita, J.S.; Moleiro, F.; Soares, C.M.M. Optimization of Metal–Ceramic Functionally Graded Plates Using the Simulated Annealing Algorithm. *Appl. Sci.* **2021**, *11*, 729. [CrossRef]
175. Taheri, A.; Hassani, B.; Moghaddam, N. Thermo-elastic optimization of material distribution of functionally graded structures by an isogeometrical approach. *Int. J. Solids Struct.* **2013**, *51*, 416–429. [CrossRef]
176. Taheri, A.; Hassani, B. Simultaneous isogeometrical shape and material design of functionally graded structures for optimal eigenfrequencies. *Comput. Methods Appl. Mech. Eng.* **2014**, *277*, 46–80. [CrossRef]
177. Abdalla, H.M.A.; Casagrande, D.; Moro, L. Thermo-mechanical analysis and optimization of functionally graded rotating disks. *J. Strain Anal. Eng. Des.* **2020**, *55*, 159–171. [CrossRef]
178. Storn, R.; Price, K. Differential evolution—A simple and efficient heuristic for global optimization over continuous spaces. *J. Glob. Optim.* **1997**, *11*, 341–359. [CrossRef]
179. Kou, X.; Parks, G.; Tan, S. Optimal design of functionally graded materials using a procedural model and particle swarm optimization. *Comput. Des.* **2012**, *44*, 300–310. [CrossRef]

180. Bertsimas, D.; Tsitsiklis, J. Simulated annealing. *Stat. Sci.* **1993**, *8*, 10–15. [CrossRef]
181. Cheng, M.-Y.; Prayogo, D. Symbiotic Organisms Search: A new metaheuristic optimization algorithm. *Comput. Struct.* **2014**, *139*, 98–112. [CrossRef]
182. Das, S.; Mullick, S.S.; Suganthan, P.N. Recent advances in differential evolution—An updated survey. *Swarm Evol. Comput.* **2016**, *27*, 1–30. [CrossRef]
183. Tsiatas, G.; Charalampakis, A. Optimizing the natural frequencies of axially functionally graded beams and arches. *Compos. Struct.* **2017**, *160*, 256–266. [CrossRef]
184. Truong, T.T.; Lee, S.; Lee, J. An artificial neural network-differential evolution approach for optimization of bidirectional functionally graded beams. *Compos. Struct.* **2019**, *233*, 111517. [CrossRef]
185. Eberhart, R.; Kennedy, J. A new optimizer using particle swarm theory[C]. In Proceedings of the 6th International Symposium on Micro Machine and Human Science, Nagoya, Japan, 4–6 October 1995; IEEE Service Center: Piscataway NJ, USA, 1995; pp. 39–43.
186. Ashjari, M.; Khoshravan, M. Mass optimization of functionally graded plate for mechanical loading in the presence of deflection and stress constraints. *Compos. Struct.* **2014**, *110*, 118–132. [CrossRef]
187. Tam, J.H.; Ong, Z.C.; Ismail, Z.; Ang, B.C.; Khoo, S.Y.; Li, W.L. Inverse identification of elastic properties of composite materials using hybrid GA-ACO-PSO algorithm. *Inverse Probl. Sci. Eng.* **2017**, *26*, 1432–1463. [CrossRef]
188. He, M.-X.; Sun, J.-Q. Multi-objective structural-acoustic optimization of beams made of functionally graded materials. *Compos. Struct.* **2018**, *185*, 221–228. [CrossRef]
189. Abo-Bakr, H.M.; Mohamed, S.A.; Eltaher, M.A. Weight optimization of axially functionally graded microbeams under buckling and vibration behaviors. *Mech. Based Des. Struct. Mach.* **2020**, 1–22. [CrossRef]
190. Wang, Z.; Sobey, A. A comparative review between Genetic Algorithm use in composite optimisation and the state-of-the-art in evolutionary computation. *Compos. Struct.* **2019**, *233*, 111739. [CrossRef]
191. Wu, C.-P.; Li, K.-W. Multi-Objective Optimization of Functionally Graded Beams Using a Genetic Algorithm with Non-Dominated Sorting. *J. Compos. Sci.* **2021**, *5*, 92. [CrossRef]
192. Nikbakht, S.; Kamarian, S.; Shakeri, M. A review on optimization of composite structures Part II: Functionally graded materials. *Compos. Struct.* **2019**, *214*, 83–102. [CrossRef]
193. Abdullahi, M.; Ngadi, A.; Abdulhamid, S.M. Symbiotic Organism Search optimization based task scheduling in cloud computing environment. *Futur. Gener. Comput. Syst.* **2016**, *56*, 640–650. [CrossRef]
194. Yu, V.F.; Redi, A.A.N.P.; Yang, C.-L.; Ruskartina, E.; Santosa, B. Symbiotic organisms search and two solution representations for solving the capacitated vehicle routing problem. *Appl. Soft Comput.* **2017**, *52*, 657–672. [CrossRef]
195. Ezugwu, A.E.-S.; Adewumi, A.O.; Frîncu, M.E. Simulated annealing based symbiotic organisms search optimization algorithm for traveling salesman problem. *Expert Syst. Appl.* **2017**, *77*, 189–210. [CrossRef]
196. Dokeroglu, T.; Sevinc, E.; Kucukyilmaz, T.; Cosar, A. A survey on new generation metaheuristic algorithms. *Comput. Ind. Eng.* **2019**, *137*, 106040. [CrossRef]
197. Do, D.T.; Lee, J. A modified symbiotic organisms search (mSOS) algorithm for optimization of pin-jointed structures. *Appl. Soft Comput.* **2017**, *61*, 683–699. [CrossRef]
198. Do, D.; Lee, D.; Lee, J. Material optimization of functionally graded plates using deep neural network and modified symbiotic organisms search for eigenvalue problems. *Compos. Part B Eng.* **2018**, *159*, 300–326. [CrossRef]
199. Yang, X.-S. Firefly Algorithm, Lévy Flights and Global Optimization. In *Research and Development in Intelligent Systems XXVI*; Springer: London, UK, 2009; pp. 209–218. [CrossRef]
200. Yang, X.-S. Firefly algorithm, stochastic test functions and design optimisation. *Int. J. Bio-Inspired Comput.* **2010**, *2*, 78. [CrossRef]
201. Yang, X.-S. Nature-inspired optimization algorithms: Challenges and open problems. *J. Comput. Sci.* **2020**, *46*, 101104. [CrossRef]
202. Li, J.; Tan, Y. A Comprehensive Review of the Fireworks Algorithm. *ACM Comput. Surv.* **2020**, *52*, 1–28. [CrossRef]
203. Lieu, Q.X.; Do, D.T.; Lee, J. An adaptive hybrid evolutionary firefly algorithm for shape and size optimization of truss structures with frequency constraints. *Comput. Struct.* **2018**, *195*, 99–112. [CrossRef]
204. Lieu, Q.X.; Lee, J. An isogeometric multimesh design approach for size and shape optimization of multidirectional functionally graded plates. *Comput. Methods Appl. Mech. Eng.* **2018**, *343*, 407–437. [CrossRef]
205. Phung-Van, P.; Thai, C.H.; Wahab, M.A.; Nguyen-Xuan, H. Optimal design of FG sandwich nanoplates using size-dependent isogeometric analysis. *Mech. Mater.* **2019**, *142*, 103277. [CrossRef]
206. Cho, J.; Shin, S. Material composition optimization for heat-resisting FGMs by artificial neural network. *Compos. Part A Appl. Sci. Manuf.* **2004**, *35*, 585–594. [CrossRef]
207. Jamshidi, M.; Arghavani, J. Optimal design of two-dimensional porosity distribution in shear deformable functionally graded porous beams for stability analysis. *Thin-Walled Struct.* **2017**, *120*, 81–90. [CrossRef]
208. Banh, T.T.; Luu, N.G.; Lee, D. A non-homogeneous multi-material topology optimization approach for functionally graded structures with cracks. *Compos. Struct.* **2021**, *273*, 114230. [CrossRef]
209. Zhang, C.; Chen, F.; Huang, Z.; Jia, M.; Chen, G.; Ye, Y.; Lin, Y.; Liu, W.; Chen, B.; Shen, Q.; et al. Additive manufacturing of functionally graded materials: A review. *Mater. Sci. Eng. A* **2019**, *764*. [CrossRef]
210. Wang, J.; Pan, Z.; Ma, Y.; Lu, Y.; Shen, C.; Cuiuri, D.; Li, H. Characterization of wire arc additively manufactured titanium aluminide functionally graded material: Microstructure, mechanical properties and oxidation behaviour. *Mater. Sci. Eng. A* **2018**, *734*, 110–119. [CrossRef]

211. Thompson, S.M.; Bian, L.; Shamsaei, N.; Yadollahi, A. An overview of Direct Laser Deposition for additive manufacturing; Part I: Transport phenomena, modeling and diagnostics. *Addit. Manuf.* **2015**, *8*, 36–62. [CrossRef]
212. Carroll, B.E.; Otis, R.A.; Borgonia, J.P.; Suh, J.-O.; Dillon, R.P.; Shapiro, A.A.; Hofmann, D.C.; Liu, Z.-K.; Beese, A.M. Functionally graded material of 304L stainless steel and inconel 625 fabricated by directed energy deposition: Characterization and thermodynamic modeling. *Acta Mater.* **2016**, *108*, 46–54. [CrossRef]
213. Qian, T.-T.; Liu, D.; Tian, X.-J.; Liu, C.-M.; Wang, H.-M. Microstructure of TA2/TA15 graded structural material by laser additive manufacturing process. *Trans. Nonferrous Met. Soc. China* **2014**, *24*, 2729–2736. [CrossRef]
214. Ghazanfari, A.; Li, W.; Leu, M.C.; Hilmas, G.E. A novel freeform extrusion fabrication process for producing solid ceramic components with uniform layered radiation drying. *Addit. Manuf.* **2017**, *15*, 102–112. [CrossRef]
215. Li, W.; Armani, A.; Martin, A.; Kroehler, B.; Henderson, A.; Huang, T.; Watts, J.; Hilmas, G.; Leu, M. Extrusion-based additive manufacturing of functionally graded ceramics. *J. Eur. Ceram. Soc.* **2020**, *41*, 2049–2057. [CrossRef]
216. Bakarich, S.E.; Gorkin, R.; Gately, R.; Naficy, S.; Panhuis, M.I.H.; Spinks, G.M. 3D printing of tough hydrogel composites with spatially varying materials properties. *Addit. Manuf.* **2017**, *14*, 24–30. [CrossRef]
217. Ren, L.; Song, Z.; Liu, H.; Han, Q.; Zhao, C.; Derby, B.; Liu, Q.; Ren, L. 3D printing of materials with spatially non-linearly varying properties. *Mater. Des.* **2018**, *156*, 470–479. [CrossRef]
218. Doubrovski, E.; Tsai, E.; Dikovsky, D.; Geraedts, J.; Herr, H.; Oxman, N. Voxel-based fabrication through material property mapping: A design method for bitmap printing. *Comput. Des.* **2015**, *60*, 3–13. [CrossRef]
219. Levy, A.; Miriyev, A.; Elliott, A.; Babu, S.; Frage, N. Additive manufacturing of complex-shaped graded TiC/steel composites. *Mater. Des.* **2017**, *118*, 198–203. [CrossRef]
220. Salcedo, E.; Baek, D.; Berndt, A.; Ryu, J.E. Simulation and validation of three dimension functionally graded materials by material jetting. *Addit. Manuf.* **2018**, *22*, 351–359. [CrossRef]